PENETRATION OF BUOYANCY DRIVEN CURRENT DUE TO A WIND FORCED RIVER PLUME

A Dissertation

by

SEONG-HO BAEK

Submitted to the Office of Graduate Studies of
Texas A&M University
in partial fulfillment of the requirements for the degree of

DOCTOR OF PHILOSOPHY

December 2006

Major Subject: Oceanography

PENETRATION OF BUOYANCY DRIVEN CURRENT DUE TO A WIND FORCED RIVER PLUME

A Dissertation

by

SEONG-HO BAEK

Submitted to the Office of Graduate Studies of
Texas A&M University
in partial fulfillment of the requirements for the degree of

DOCTOR OF PHILOSOPHY

Approved by:

Chair of Committee,	Robert D. Hetland
Committee Members,	Achim Stössel
	Steven F. DiMarco
	Fuqing Zhang
Head of Department,	John Morse

December 2006

Major Subject: Oceanography

ABSTRACT

Penetration of Buoyancy Driven Current Due to
a Wind Forced River Plume. (December 2006)
Seong-Ho Baek, B.S., Naval Academy, Republic of Korea;
M.S., Advanced Institute of Military Science and Technology, Republic of Korea
Chair of Advisory Committee: Dr. Robert D. Hetland

The long term response of a plume associated with freshwater penetration into ambient, ocean water under upwelling favorable winds is studied using the Regional Ocean Modeling System (ROMS) in an idealized domain. Three different cases were examined, including a shore perpendicular source and shore parallel source with steady winds, and a shore perpendicular source with oscillating alongshore winds.

Freshwater flux is used to define plume penetration. Alongshore penetration of buoyant currents is proportional to freshwater input and inversely proportional to upwelling wind stress strength. Strong wind more quickly prevents fresh water's penetration.

Under upwelling favorable winds, the plume is advected offshore by Ekman transport as well as upcoast by the mean flow. This causes the bulge to detach from the coast and move to upcoast and offshore with a 45 degree angle. The path of the bulge is roughly linear, and is independent of wind strength. The bulge speed has a linear relationship with the wind stress strength, and it matches the expected speed based on Ekman theory.

Sinusoidal wind leads to sequential upwelling and downwelling events. The plume has an asymmetric response to upwelling and downwelling and fresh water flux is

changed immediately by wind. During downwelling, the downcoast fresh water transport is greatest, while it is reduced during upwelling. Background mean flow in the downcoast direction substantially increases alongshore freshwater transport.

DEDICATION

To my lord, Jesus Christ,

to my family, Kim Sunkyung and Irene Baek,

to my parents, Baek, Unhwan and Kim, Youngsoon,

to R.O.K Navy

for their endless love and support.

ACKNOWLEDGEMENTS

I am grateful to my dissertation advisor, Dr. Robert D, Hetland. He showed me how to approach, research, develop logic and writing techniques. Dr, Hetland's intuitive thinking brought development of ideas to me. He make my dream come true. I am indebted to Dr. Achim Stössel. He always paid attention to my words and encouraged me to achieve the goal by gentle and great recommendations. His help was invaluable to me. I am indebted to Dr. Steven Di, Marco and Dr. Fuqing Zhang for their help to develop logical thinking and for their generous advice and unflagging encouragement.

I also gained enormous help from Dr. Steve Baum. Especially, I shall never forget his amazing rescue when I developed big computational trouble. A thousand thank-yous are due. My thanks go also to all the people in the Oceanography Department for their help and care. I am thankful to my family for their patience and forgiveness.

I know who lead me from the start to this point. When I was frustrated by unavoidable circumstance and fell in trouble by the language barrier, I know who stood by me and supported me. Thank you my Lord.

I can do everything through him who gives me strength *(Philippians 4:13)*

TABLE OF CONTENTS

Page

LIST OF FIGURES

FIGURE Page

LIST OF TABLES

CHAPTER I

INTRODUCTION

1. Motivation

River plumes have recently been the subject of much study due to coastal environmental pollution problems related with the coastal ecosystem. Sewage, industrial waste and excess fertilizer is transported from the land to continental selves by rivers. It may cause serious damage to the coastal ecosystem through eutrophication. For example, seasonal hypoxia on the Texas-Louisiana continental shelf is associated with excess nutrients from and a stratification caused by the Mississippi and Atchafalaya Rivers (Rabalais et al., 1996).

River water inflow to the coastal ocean leads to strong stratification that prevents oxygen supply by suppressing mixing between the surface and bottom layers. In addition, organic matter from high production in the surface layer due to the excess nutrients in the river may cause high oxygen consumption in lower layer, as organic material falls down from the surface layers. Low dissolved oxygen levels may lead to a loss of aquatic habitat (Rabalais et al., 1996).

In the northwestern Gulf of Mexico, hypoxia is generated only during summer season. During the nonsummer season, the wind blows down coast and drives river water to the south along the coast. But in the summer season, the wind changes to upcoast and river water is trapped from spreading along the coast, creating a freshwater

This dissertation follows the style and format of *Journal of Physical Oceanography*.

pool (Morey et al., 2005). This pooling of fresh water creates conditions that favor hypoxia because of strong stratification over the shelf during summer. Thus, to understand the mechanism of hypoxia over the Texas-Louisiana shelf, we need to first understand Texas-Louisiana shelf circulation pattern and the distribution of fresh water over the shelf.

The Texas-Louisiana shelf, in northwestern Gulf of Mexico, is strongly affected by river discharge. This area receives one of the largest discharges of fresh water through the Mississippi-Atchafalaya River system (Dunn, 1996). Roughly 53% of the total Mississippi River flux discharges onto the Texas-Louisiana continental shelf (Dinnel and Wiseman, 1986). The Texas-Louisiana shelf's circulation is influenced by various factors: wind, tide, river discharge, loop current eddies detached from the eastern Gulf of Mexico loop current and so on. It has been found that wind is the most important factor in determining circulation on the inner Texas-Louisiana shelf when hypoxia is found (Cochrane and Kelly, 1986; Wang, 1996; Cho, 1996).

Seasonally changing wind direction leads to specific circumstances in Texas-Louisiana shelf. Cochrane and Kelly's (1986) first comprehensive description of the seasonal circulation scheme based on the M/V GUS III 1963-1965 hydrographic data show that during nonsummer season, from September to June, cyclonic circulation is dominant pattern in mid self region and during summer season, July to August, anticyclonic circulation is dominant (Figure 1). Near shore flow of the Texas-Louisiana shelf is a typical example of the wind driven coastal jet (Cochrane and Kelly, 1986) and the Texas-Louisiana inner-shelf currents are strongly coherent with the alongshore wind component (Cochrane & Kelly, 1986 and Wang, 1996).

During the nonsummer season, the wind direction is downcoast and drives the alongshore current on the inner shelf. Here, downcoast is defined as the direction of westward shelf wave propagation**.** The alongshore current distributes Mississippi-Atchafalaya river water downstream near the south Texas coastal region. Downcoast near shore flow is strongly affected by 2 factors. It is driven by downcoast along shelf wind and enhanced by Mississippi-Atchafalaya River water discharge.

During summer season from July to August, the wind direction is changed to counter direction and average wind has an upcoast component. Upcoast is against the direction of shelf wave propagation, or eastward. This leads to an anticyclonic circulation in the mid shelf as the nearshore flow is halted or reversed by the wind (Li et al., 1996; Li et al., 1997; Cho et al., 1998). The mean flow prohibits downcoast spreading of river water and made fresh water pool in the Texas-Louisiana shelf. So, to understand generation mechanism of freshwater pool in the Texas-Louisiana shelf related with plume, it is necessary to study the reaction of plume and resulting buoyancy driven current under the upwelling conditions.

2. Previous studies

Previous numerical studies have typically divided the plume into two parts; bulge and alongshore current. The bulge, the anticyclonic turning flow is generated by large scale river water discharge into the shelf with saltier and denser sea water in the Northern Hemisphere (Garvine, 1987). Alongshore current, the baroclinic boundary current propagates in a narrow zone along the coast as a coastal Kelvin-wave (Wiseman et al., 1976; Chao and Boicourt, 1986; Wiseman and Dinnel, 1988; Oey and Mellor,

1993; Brooks, 1994; Chapman and Lentz, 1994).

Garvine (1995) suggests classification of river plumes based on the Kelvin. The Kelvin number is defined as the ratio of the externally specified width of the flow (for example, the width of an estuary mouth, to the baroclinic Rossby radius deformation; $\sqrt{g'H}/f$ where g' is reduced gravity, H is the mean buoyant layer depth and f is Coriolis parameter is used as indicator for measuring the importance of rotational effect to categorize river plumes. He classified by two limiting cases, K<<1 or small-scale discharge and K>>1 or large scale discharge.

Yankovsky and Chapman (1997) also adopt plume classification criterion with the vertical structure. They sorted river plumes as 3 types, surface-advected, bottom-advected and intermediated plume. In the surface-advected plume case, the plume does not interact with the bottom. In the bottom-advected plume case, the plume is trapped in a particular depth because the lateral density gradients within the front create a vertical shear. The flow adjusts by moving offshore until the flow is zero at the bottom. Thermal wind shear at the front thus determines critical limit of the plume's further offshore movement. In the intermediated plume case, the plume has mixed character of before two cases. Characters of each types of plume are determined by grouping of non-dimensional parameters, Burger number: S and the Rossby number: Ro (Influence of stratification can be measured by the Burger number and rotation effect can be measured through the Rossby number). Generation condition of surface-advected plume is $S > (2Ro)^{1/2}$ where $S = \sqrt{g' h_o / fL}, Ro = v_i / fL$, g' is reduced gravity based on the inflow density anomaly, h_o is the inflow depth, v_i is the inflow velocity, f is the Coriolis parameter and L is the inflow width. Bottom-advected plume case is based on small S

(ambient water and inflowing water have similar densities). Intermediate plume case is produced in between both conditions. In addition, they show that inflow velocity level can not give any effect to establishment of intermediate and surface-advected plume under the large density difference condition.

As the freshwater inflow volume increases, river plume's inflow velocity into the surrounded salty water also increases. Oey and Mellor (1993) and Chapman and Lentz (1994) investigate these intrusion velocities. Whitehead and Chapman (1986), Chao and Boicourt (1986), Chao (1988) mention that intrusion velocities shrink due to bottom friction. The buoyancy driven gravity current can flow several hundreds of kilometers distance range from the source along the coast until it dissipates and completely mixes with the ambient water (Munchow and Garvine, 1993).

From generation to dispersion of plume under the upwelling favorable wind condition has been studied by observation (Fong et al., 1997; Hickey et al., 1998; Rennie et al., 1999; Johnson et al., 2001; Sanders and Garvine, 2001; Hallock and Marmorino, 2002; Johnson et al., 2003; Houghton et al., 2004) and several modeling studies concerned with upwelling favorable winds to characterize the response of plumes (Chao, 1988; Kourafalou et al., 1996; Xing and Davies, 1999; Austin and Lentz, 2002; Berdeal et al., 2002; Whitney and Garvine, 2005).

Hetland (2005) studied water mass structure of sinusoidal wind forced river plumes by using an idealized numerical model with fresh water discharging from an estuary into a continental shelf. He suggested that the plume can be divided into two different dynamical regions and those are presented by the difference of dominant mixing. In the near-field advective shear mixing is dominant but in the far-field wind

mixing is prevailing. In the near-field strong mixing occurs and strongest wind mixing take place under the upwelling wind condition. The changing plume position is reflected in the wind stress forcing cycle. The plume loses contact with the coast as it is blown to the offshore by the upcoast (upwelling) wind stress and the plume is shifted downcoast during down coast (downwelling) wind.

Lentz (2004) describes the response of a plume to upwelling-favorable winds as developing of a two-dimensional theory that includes entrainment. Fong and Gayer (2001) focus on river plume's offshore spreading under the upwelling-favorable condition through model simulation in a three-dimensional rectangular domain. They show that the plume is advected offshore by the cross-shore Ekman transport and the plume become wider and thinner by the cross-shore Ekman currents and they suggest that in modifying the shape of the plume, the advective processes are important.

3. Goal of this study

Most previous idealized studies focused on short term plume response and do not deal with long term plume response associated with penetration problem. There are a few notable exceptions like Garvine (1999), Yankovsky and Chapman (1997).

The main question is how far fresh water can penetrate downcoast under upwelling favorable wind conditions and what factors affect this penetration?

The penetration problem without wind forcing was studied by Garvine (1999) through an ideal model study. He show plume's penetration is affected by inflowing source and shelf bottom slope. Increased shelf bottom slope shortens the alongshore penetration. However, penetration of wind forced plume was not considered by Garvine.

Fong (2001) studied the response of a river plume during an upwelling wind event. He focused on offshore advection of a plume due to the Ekman transport in a short-term model run, but not considered relationship with penetration.

Hetland (2005) discusses the plume's movement in response to changing wind stress. During upwelling, the plume loses contact with the coast and during downwelling, the plume is pressed against the coast, developing a strong coastal current. But reaction to mean flow and sinusoidal wind with mean flow and alongshore freshwater flux variation are not studied.

Better understanding of plume penetration along the coast can help to predict the pathways of fresh water and the along shore penetration of river waters. Additionally, understanding the river water expansion processes into the ambient salty water can help us to understand the coastal ocean circulation through improving of the knowledge of the wind forced river plume and correlation with the resulting buoyancy driven current.

So, the aim of this study is to describe the fresh water penetration in ambient saltier water under upwelling favorable-wind and to investigate relationship with the plume detaching from the coast through the numerical model in an ideal case.

CHAPTER II

NUMERICAL SETUP

1. ROMS (model)

The Regional Ocean Model System version 2.1 (ROMS, Haidvogel et al., 2000) is used for the simulations presented below. ROMS is based on the S-coordinate Rutgers University Model (SCRUM) described by Song and Haidvogel (1994). ROMS solves hydrostatic, Boussinesq, primitive equation with potential temperature, salinity, an equation of state. ROMS can be configured to include point sources of buoyant.

The model uses a split-explit time-stepping scheme to solve the momentum equations. In the vertical, the discretized coordinate system uses stretched terrain-following coordinates. Vertical equations are solved implicitly using a tridiagonal method. Horizontal grid uses orthogonal curvilinear coordinates on a staggered Arakawa C-grid. (Haidvogel and Beckmann, 1999). ROMS has a number of choices for advection scheme and vertical mixing parameterization through the modular code design.

2. Shore perpendicular source

Numerical configuration setup generally follows Hetland's (2005) idealized river plumes model study focused on relating plume structure to vertical mixing.

A rectangular domain consists of an unvarying shelf slope, straight coast line, and an estuary perpendicular to the coastline where river water is introduced into the domain. Whole domain size is about 300km length north to south and 219km width west

to east. Straight coast line runs across from north to south on the west side of domain. An estuary is embedded within the coastline. The estuary is 27km length, 11km width and round shape bottom with 10m maximum depth. So, domain size of the coastal ocean is about 300km alongshore, and 192km cross-shore. Only the western boundary is closed by land. Other boundaries are applied open boundary condition. An Orlanski radiation condition is used for extrapolating the interior solution at the boundaries. A sponge layer, a region of increased horizontal viscosity near the open boundaries, is used to suppress computational noise related with the radiation (Palma and Matano, 1998). To relax model data towards the idealized background state, a nudging term is added to equations of tracers by adaptive nudging technique. When the waves are directed inward at the boundary, the boundary is active and for outward fluxes the boundary is passive (Marchesiello et al., 2001). Nudging is specified to be larger when the boundary is active. For barotropic flow boundary conditions, a Flather (1976) condition is used.

Bottom slope from cost to offshore the minimum depth is 3m at the coast and depth of continental shelf is uniformly increase to offshore with 1/2000 linear rate. The maximum depth is about 97m in the eastern edge of domain (Figure 2). Depth at the coast is selected as shallower depth than maximum depth of estuary, so there is a cut in the shelf bathymetry due to the estuary.

A rounded cross-channel estuarine topography gives more robust numerical solutions than rectangular flat bottom estuary. In a rectangular, flat-bottomed estuary, the along-channel salinity structure is affected by numerical noise, in which there are grid-scale oscillations in the bottom salinity along-channel. The grid-scale noise creates artificial unmixing generated by numerical over and under shoots, since the saltier water

stays on the bottom, but the fresher water rises (Hetland, 2005). By changing estuary bottom shape from a square type to a round type this numerical noise is suppressed.

The numerical grid is focused around the point of estuarine outflow. Higher resolution is specified alongshore coast and near the estuarine river water outflow region than any other area (Figure 2). On contrast near boundaries resolution is much coarser. It can give us more precise observation of plume motion and increase domain size and reduce grid scale noise at the boundaries.

Initially the model is assumed to have a flat surface, no flow and uniform salinity of 32 psu through whole domain. Vertical temperature stratification analytically stabilized 20ºC in 10m homogeneous mixed layer and exponentially decreasing in depths, and initial condition in bottom layer is 5ºC. The whole domain is rotating uniformly with $f = 10^{-4} s^{-1}$. Second order horizontal mixing is used in both momentum and tracer. Fourth-order Akima horizontal, vertical advection applied for tracer and Mellor/Yamada level-2.5 closure applied for vertical turbulence mixing (Mellor and Yamada, 1982).

Between 1000 and 7000 $m^3 s^{-1}$ fresh water ($\rho = 0$) flux are introduced into the model domain on westward end of the estuary and spatially uniform along shore wind with amplitude of 0.1 to 0.5×10^{-4} m^2 s^{-2} forced the domain as surface momentum stress (Figure 3). Forces, fresh water and wind, are applied through ramps with the hyperbolic tangential function. Those are increase from 0 to the final steady value. Fresh water's ramping time scale is 4days and that of wind is 3days. Therefore freshwater inflow begins at the start point and increase the volume after 4 days. 4 days later the volume maintains certain amount. Wind starts to blow from 2nd day toward the north and linearly

increase until 5th day than maintain steady force (Figure 4). The model is integrated from between 1 to 2 months.

3. Shore parallel source

The shore parallel source runs introduce fresh water into an estuary that is parallel to the coast instead of perpendicular as described in the previous section. This model's setup is generally same with the shore perpendicular source model except to change to the domain. Freshwater inflow is introduced from the northern estuary, and upwelling wind is again applied through whole domain (Figure 5).

East and south boundaries of the domain are open sea with unvarying shelf slope but north and west are surrounded by land with straight coastline. Estuary located in the west corner of north coast. It has 12m maximum depth, 10km length, 9km width and rounded bottom (Figure 6).

The numerical grid is formatted in a similar way as the shore perpendicular source model. Resolution concentrated near the estuary and along the coast (Figure 6). The domain length is 320km, width is 218 km with linear bottom slopes to the north and west of 1/2000. Minimum depth is same with the previous, 3m at the coast, but the maximum depth is limited as 30m for numerical integration speed. This does not strongly affect the solution because the alongshore current is trapped on the surface layer due to the density difference and flow along the coast so, deeper layer water will not interact with the alongshore current (Figure 6). Surface layer temperature initialized with mixed layer temperature and set up as 20ºC and exponentially decreasing in depths, at the bottom layer it is 10ºC.

The fresh water flux is initially zero, and increases to 5000 $m^3 s^{-1}$ during 6 days then is kept uniform. Wind stress also begins at zero. The wind increases from 4^{th} day to $0.1x10^{-4}$ m^2 s^{-2} amplitude until the 7^{th} day, after which it maintains the same stress (Figure 7). The model test period is much longer than shore perpendicular source case. This simulation lasted 12 months. The shore perpendicular cases each lasted 2 months.

CHAPTER III

RESULTS

1. Shore perpendicular results

The no forcing case shows a bulge and alongshore current as discussed previously. As freshwater leaves the estuary, it turns anticyclonically forming a bulge south of the estuary mouth then flows to the south along the coast as a coastal Kelvin-wave (Figure 8). Define the “downcoast” direction as south here in the direction of Kelvin wave propagation. Both the bulge and the jet are general features of steady state coastal plumes in ideal model observed in many other studies (Garvine, 1987; Wiseman et al., 1976; Wiseman and Dinnel, 1988; Oey and Mellor, 1993; Chapman and Lentz, 1994). However, under the upwelling favorable wind conditions, the features of the plume are much different.

Upwelling winds causes the ambient surface currents flow to upcoast, as a coastally trapped jet, and to offshore due to Ekman transport. The plume is affected by both. Upwelling favorable wind leads the plume to detach from the coast and to move to offshore. Both processes prevent downcoast freshwater penetration into the ambient salty water.

I will discuss plume detachment in more detail later, here I will focus on plume penetration. Initially, fresh water directly flows into the shelf through the estuary located on the west coast then the plume is established in salty water with anticyclonically turning flow and an alongshore current under zero wind conditions. After 2 days, a

northward upcoast upwelling favorable wind is applied throughout the domain and the plume starts to move to offshore. The alongshore current's progress to the south is arrested by the wind.

10 days later the bulge is move more to the northeast and detaches from the coast. When this happens, the alongshore current cannot flow to the south at all. After the bulge detaches from the coast, a new, second bulge forms. Thus, the inflow is separated into two parts, one part continuous to supply for the original bulge and the other part seeds the newly formed second bulge (see Figure 9).

As the bulge detaches more from the coast, Returning flow, alongshore current return to the recirculation zone of plume, become strong and form small cyclonic rotation. These aspects happen within 1 month run under $3000\,m^3 s^{-1}$ fresh water source and $0.1\times10^{-4}\,m^2 s^{-2}$ wind stress applied condition.

After 1.5 month, cyclonic returning flow suddenly reacts with the second bulge and quickly merges with the bulge. The second bulge causes fluctuation and distorts original bulge. Eventually the whole plume is dissipated. Figure 10 shows the time sequence described here.

Freshwater flux is used to define plume penetration. Plume extension can be estimated through observation of alongshore boundary between freshwater and ambient salty water and the boundary can be described by freshwater flux. So, alongshore freshwater flux variation is used to present plume penetration ratio.

Definition of freshwater flux is.

$$Q_f = \iint \frac{S_o - S}{S_o} v\,dx\,dz \qquad (1)$$

where, S_o is the ambient salty water salinity ($\rho = 32$), S is alongshore current salinity, v is averaged speed of alongshore current cross section $dxdz$ and Q_f is averaged fresh water flux.

Freshwater flux is a good metric for measuring plume penetration quantitatively and qualitatively because in this model no other freshwater source exists than estuary and it seems to fit well with other aspects of the plume, such as surface salinity. Additionally, it presents movement of both waters, fresh and saltier, by included vector velocity of flow.

In this study, the front is defined as the southern boundary between fresh water and ambient salty water.

Variation of front position can be presented by alongshore zero freshwater transport flux.

Where southward fresh water volume transport exists, the plume flows to the south, and when the fresh water flux value is positive, $Q(x_3) > 0$, there is northward volume. At the front, freshwater flux becomes zero (Figure 11).

In Figure 12, near the estuary and far from the estuary, freshwater fluxes are positive values and mid distance from the estuary freshwater flux is negative. The first zero point, the turning point of flux from positive value to negative value, is the boundary between the bulge and alongshore current. Before the zero crossing point, near by the estuary, flux has positive value by alongshore current returning flow to recirculation zone of plume but after the zero crossing point the plume flows to the south. The second zero crossing point, the turning point of flux value change negative to positive, defines the fresh water penetration distance.

The second zero crossing point changes location in time. As shown in figure 12, the distance between estuary and the crossing point becomes smaller in time. At the beginning, before wind blows, the front moves to the south because of the southward flowing alongshore current. But after the wind starts to blow, the front moves to the north until it is near the estuary. That means, as fresh water is pushed up to near by the estuary, as northward freshwater alongshore volume transport becomes dominant. This shows northward mean flow generated by upwelling wind is enhanced in time.

Alongshore penetration of buoyant currents is proportional to freshwater input and inversely proportional to upwelling wind stress strength. As increasing freshwater inflow fronts are more moves to the south but as increasing wind stress fronts are located more north. Thus, lots of freshwater inflow causes the freshwater to penetrate further into the salty water, but strong upwelling wind prevents fresh water penetration into salty water. This is shown by examining the movement of the front in time. Front speeds are calculated by plotting of along-shore zero flux points in the time verse along shore distance (Figure 13).

Strong wind lead faster movement of surface water so, it is expected that strong wind has positive relationship with the front moving speed. However, front moving speed decrease exponentially by increasing wind stress and eventually converge to the zero. This is because strong winds allow less fresh water penetration into the salty water at the early stage, so there is less reduction in the penetration distance with increasing wind stress. Eventually, under the strongest wind condition, the fresh water almost cannot penetrate at all into ambient salty water so, front moving speed become nearly zero. That means strong wind quickly prevents fresh water's penetration by faster set up

of the strong front near by the estuary than weak wind (Figure 14, Table 1).

2. Shore parallel results

As mentioned above, the plume has two parts; the bulge and alongshore current. Shore perpendicular results show bulge is important in determining the plume structure under upwelling wind condition because much of the freshwater is stored in the bulge. When a front moves northward, the plume is detached from the coast and bulge moves offshore.

Now, we examine quantitatively and qualitatively how the bulge affects the solution by comparing with the shore perpendicular source.

Shore parallel source model set up is similar to previous plume model, except that the domain includes north wall and north estuary (Figure 6). However, one of different arrangements with this plume model is adjusting the inflow ramping time scale in order to reduce bigger spurious salt flux. Artificial 'unmixing' creates a pool of salty water along the sea floor, as well as a spurious source of fresh water near the surface. Spurious salt estimated follow based on Hetland (2005).

$$v_f = \int_0^\tau Q_f dt = \iiint (\frac{S_o - S}{S_o}) dv$$
$$v_{fclip} = \iiint (\frac{S_o - S_{clip}}{S_o}) dv \qquad (2)$$
$$\text{where} \quad S_{clip} = \min(S, S_o)$$

Volume of fresh water (v_f) is integration of fresh water flux (Q_f) and it can be calculate through the changing rate of salinity in domain. The 'clipped' fresh water

volume also can be calculated same way, except that spuriously high values of salinity are clipped to the original background value. The clipped fresh water volume is always larger or at least same as, the fresh water volume, $v_{fclip} \geq v_f$. So, the percent of spurious fresh water formation is given by $\left(v_{fclip} / v_f\right) - 1$.

To reduce this spurious salt flux, round shape estuary bottom was used and fresh water flow into the domain through the ramp with the hyperbolic tangential function like previous plume model and ramping period is in tuned. Longer ramping time scale generates smaller spurious error (Figure 15). 6 days time scale which is 2 days longer than shore perpendicular model is adjusted and other conditions are same.

No forcing case alongshore current dose not form a bulge, and only flows to the south like Kelvin wave. In time, the model generates a stable alongshore current. With upwelling favorable wind, the whole fresh water flow is offshore along the northern coastline, without significant southward penetration, and front is very stable in time. Nevertheless, it's position various wind strength.

Before the wind blows, the current flows to the south along the coastline like a Kelvin wave. After wind stress is applied, the current is pushed up to the north without further penetrating to the south and all fresh water flows to offshore and along the northern coast. As the wind stress increase the front withdraws more to the north. It is the same phenomenon that was discussed above with the shore perpendicular source in the alongshore current portion of the plume south of the bulge. The present model is different because, after wind force becomes stable, the current also no more pushed up to the north and the front become stable (Figure 16). This phenomenon is same under the various wind strength. In figure 17 we can see the front is stable during and entire 12

month simulations.

Movement front strongly related with the movement of bulge**.** Shore parallel source model result show that front stability and movement strongly related with the plume stability and movement accompanied with detachment.

Shore perpendicular source case front is located much closer distance from the estuary than shore parallel source case because shore perpendicular source case much smaller portion of freshwater transport to the south than shore parallel source case as big portion of freshwater is trapped in bulge.

3. Motion of bulge centroid

As preceded work it is need to choose a tracking method of bulge to find out detachment rate of the bulge from the coast and its moving path. The no wind forced plume case some of portions of inflowing fresh water are transported through alongshore current and other large portions of fresh water remain in the bulge. The bulge grows in time. The wind forced plume, however, the bulge is grows faster than the no wind case by inflowing fresh water plus along shore current returning flow to the bulge. So, it is not a good method to estimate detachment of the bulge by the distance or fresh water flux variance between the coast boundaries of the bulge neared coast. Because fresh water cover most around coast area, it is not easy to recognize boundary of bulge. So, bulge center tracking is proper way to find out detaching rate from the coast and moving pattern than bulge boundary tracking.

Highest surface point of plume is well present center of plume.

Horner-devine et. al. (appeared) defined the bulge centre as zero-crossing in

velocity profile but in this study, it is defined other approach. Boundaries are discerned sharp changing point of salinity and surface height. Based on boundary, the middle point of bulge is chosen as the center of the plume but to simplify tracking work uncomplicated define is used.

Based on boundary define, to concern the lowest salinity point as a bulge center is not proper because fresh river water flows along a rim of the plume respectably center salinity is higher than boundary. However, to select the highest surface point of plume as the center of the plume is well match the middle point of the bulge. That is reasonable define stand on geostrophic balance. Center of anticyclonic bulge has highest surface height than any others (Figure 18).

When the bulge detaching from the coast it behaves like a slab and move to upcoast and offshore with 45 degree angle.

Groundwork of definition, bulge moving patterns are observed. Before a wind blow, a plume generated by inflow and after applied the wind stress the plume shapes modified by the wind. At early stage bulge moving path drawn on bulge center positions show a parabolic curve than change to linear line in time (Figure 19). The duration from start to turning points, spending time to change path from parabolic curve to linear line, depend on the strength of wind stress. Under the strong wind, the time duration is shorter than weak wind case. Eventually bulge move to the northeast with almost 45 degree angle (Figure 19). Because the mean flow driven by upwelling wind make bulge move to upcoast and simultaneously Ekman transport move bulge to offshore combined both movements move the bulge to northeast with almost 45 degree angle.

Addition to, When the bulge detaching from the coast it behave like a slab

because the plume move on Ekman transport layer without changing of thickness.

Nevertheless of various wind strength, all flow are same path. Linear plume moving path is independent of the wind stress strength and all flows move to same way. It is clearly showing in Table 2. All lines presented path have very similar values 1. It means path angle is 45 degree.

Simulated the bulge moving speed is linear and well match the expected speed. Simulated the bulge moving speeds are calculated through distance from the estuary to center of the plume. Calculation of the expected rate, moving speed, is based on Ekman theory. The plume stay on the upper layer and move by the Ekman transport because the Ekman balance is main component of alongshore momentum (Fong et al., 1997). Under the spatially uniform wind stress condition through whole model domain, the integral of continuity equation over upper layer give $uh =$ constant. It makes imagine that without change of thickness plume detach from the coast and move to offshore with some speed by Ekman balance.

$$u = \frac{\tau^y}{\rho f h} \tag{3}$$

Where h is the thickness of plume, ρ is the mean density of plume in upper layer, τ^y is alongshore direction wind stress and f is Coriolis parameter. To compare model and expected result critical depth is calculated based on Hetland (2005).

$$h_c = \frac{2\tau}{\rho_o f}\sqrt{\frac{Ri_c}{h_f g \Delta\rho_f / \rho_o}} \tag{4}$$

$$h_c = \left[\frac{4Ri_c \left(\frac{\tau}{\rho f} \right)^2}{g \frac{\Delta\rho}{\rho_o}} \right]^{1/3} \quad (5)$$

where $h_f = \int_{-H}^{\eta} \frac{s_o - s}{s_o} dz$ and

Bulk Richardson number, $Ri = \Delta\rho g h / \rho_o \Delta u^2$.

Hetland's (2005) calculations of critical depths, equation (4) are very similar with Fong and Geyer's (2001) estimation, equation (5). Even though each other study deal with different dimensional model. They show plume thickness only affected by wind stress, initial condition and Ri_c, critical Bulk Richardson number and critical depth, the plume thickness at the seaward front, used to calculate plume's spreading offshore speed in Fong and Geyer (2001) because plume is keep up constant thickness and width during moving offshore. In this study plume thickness is not much changed and the width is maintained generally 3 times bigger size than deformation radius. Therefore, plume thickness at the seaward front is can be said critical depth in this study too and at that depth have maximum N^2 value.

Those expected speed is based on fixed thickness of plume. Both are very similar value but have a litter gap. Calculated depth through model has small variation of thickness. Generally, under weak wind model calculation plume detaching speed is smaller than expected speed but under strong wind condition it show counter result. That means in the strong wind condition simulated depth is deeper than critical depth and it lead smaller detaching speed of model result than expected speed (Table 3). Because

strong wind enhance shear mixing through strong wind more stirring in the upper layer Ekman flow (Hetland 2005).

Results of above plume moving speed calculation show us that linear plume moving speed nevertheless various wind stress and simulated detaching speeds (thin line) from the coast are very similar with expected detaching speeds (thick line) calculated from equation (3) (Figure 20).

Bulge moving speed has linear relationship with the wind stress strength.

Plume moving speed has linear relationship with the wind stress. That means as increase wind stress plume's moving speed also linearly increase (Figure 21).

Result of combine movement of front and plume against wind stress present to us that strong wind allows small budge of front through faster moving of plume to northeast. It lead rapid prevent fresh water penetration. Weak wind let the front move to longer distance through slower plume movement and its permit more penetration of fresh water to ambient water by time-consuming prevent fresh water. Consequently, plume's movement causes to withdraw of front to the north and detachment rate of plume coherent with alongshore front movement (Figure 22).

4. Sinusoidal wind

Above model results show reaction of plume to wind. How much response to wind and what about affect of ambient water flow and relationship with the alongshore fresh water flux? To get answer the question it is need to apply blowing direction changing wind in time and ambient water flow. To present critical changing wind direction sinusoidal function is selected and for steady ambient water mean flow is

applied. To compare with the result of plume model, it is tested in same domain, configuration and input parameters.

3000 $m^3 s^{-1}$ fresh water ($\rho = 0$) flux are uniformly forced in through the estuary like plume model and sinusoidal along shore wind with amplitude of 0.5×10^{-4} m^2 s^{-2} forced as surface momentum stress. Both forces time-series applied with a ramp to reduce generation of high frequency oscillations. Fresh water flux forced with the hyperbolic tangential function. It is increase from 0 to the 3000 $m^3 s^{-1}$ during 4days then maintains volume. Sinusoidal wind has about 6.6 days cycle (Figure 23). Addition to, southward mean flow $0.05\, ms^{-1}$ added.

When $0.05\, ms^{-1}$ southward mean flow only applied model domain plume is restricted by mean flow without extend to north and offshore in time. Plume shape also is changed from a circular to an ellipse by push to the coast and along shore current flow also increase (Figure 24).

The plume moves onshore and offshore in response to changing wind direction. Sinusoidal wind leads upwelling and downwelling as changing of wind direction by Ekman transport and the plume show asymmetric response.

During downwelling transport is become greatest and during upwelling it is become so litter. During upwelling plume detached from the coast and along shore flow become weak and for downwelling period plume pushed to the coast and along shore flow enhanced (Figure 25).

Background mean flow substantially increases alongshore freshwater transport. In sinusoidal wind with southward mean flow, mean flow is work as subsidiary force to boost or reduce upwelling and downwelling. For the duration of downwelling, plume is

more pushed to the coast and form strong alongshore current. Mean flow make enhance all. However, during upwelling event, plume is less detached from the coast than sinusoidal wind only forced case and southward alongshore flow is not much decrease like sinusoidal wind only case. It is due to reduce of wind effect by counter flowing mean flow (Figure 26). It is presented clearly by figure 27 and 28.

4 case of different force model result included static state plume case (Figure 29, 30) suggest calculating alongshore fresh water flux by case to understand relationship with the wind.

Fresh water fluxes are calculated based on Hetland (2005) at the 80km distance across shore line from the estuary. Figure 31 present averaged fresh water flux under different forcing and no forcing case.

Both sinusoidal wind case and sinusoidal wind with mean flow case have same cycle 6 days. It is shorter than wind stress cycle 6.6 days.

The plume has an asymmetric response to upwelling and downwelling and fresh water flux is changed immediately by wind. So, alongshore transport may be modified by order one under the wind stress.

Downwelling transport is great. Especially, wind with mean flow case northward transport decrease to almost zero. Therefore freshwater penetration prevent by upwelling favorable wind. It is concur with the plume model result. In sinusoidal wind with mean flow case fresh water flux is higher value than no mean flow sinusoidal wind case. It means flow work as enhance force to alongshore fresh water flux.

CHAPTER IV

DISCUSSION

Hypoxia on the Texas-Louisiana continental shelf in the northwestern Gulf of Mexico is associated with a strong stratification caused by the Mississippi and Atchafalaya Rivers and seasonal changing wind. It is generated only during summer season because the Texas-Louisiana shelf circulation pattern is changed during summer season due to changing wind direction.

During the nonsummer season, the wind direction is downcoast and drives the alongshore current on the inner shelf. The alongshore current distributes Mississippi-Atchafalaya river water downstream near the south Texas coastal region. However, during the summer season, the wind direction is changed to upcoast, leading to an anticyclonic circulation in the mid shelf. The mean flow driven by the wind prohibits downcoast spreading of surface trapped fresh water, creating a freshwater pool over the Texas-Louisiana shelf. This fresh water pool creates conditions to hypoxia by creating of strong stratification over the shelf during summer season. Strong stratification prevents oxygen supply by suppressing mixing between the surface and bottom layers. Loss dissolved oxygen in the lower layer of the water column causes loss of aquatic habitat (Rabalais et al., 1996).

This study of the reaction of plume and resulting buoyancy driven current under the upwelling conditions through a simplified rectangular ideal model helps us to understand the generation mechanisms that cause the summer-time freshwater pool to be

formed over the Texas-Louisiana shelf.

The shore perpendicular model with a narrow estuary demonstrates how a thin plume moves offshore through Ekman layer transport under upwelling wind. This response helps us to understand the relationship freshwater penetration rate into ambient salty water with movement of the plume consisted with a bulge and current. This configuration has a large Burger number ($S = \sqrt{g'H} / fL$) and large Rossby number ($R_o = v / fL$), so, it can be classified as a surface-advection or intermediate plume (Yankovsky and Chapman, 1997).

Because the channels of the Mississippi River are narrow, and the discharge is large, the Mississippi River has a large *S* and *Ro*. The flow out of Southwest pass, the largest distributor in the Mississippi delta, forms an anticyclonic bulge and alongshore flow. This plume spread offshore with little contact to the bottom, because buoyant freshwater remains in the surface without mixing with the ambient salty water. Thus, the Mississippi River Delta outflow generates a surface-advected or intermediate plume with large *S* and *Ro.*

Because the mouth of Atchafalaya bay is large, the Atchafalaya River is characterized by small *S* and *Ro.* Atchafalaya River also flows into the shelf perpendicularly, with flow along the coast turning anticyclonicly. Near the mouth, the plume covers the whole water column, and is in continuous contact with the bottom. Its behavior is controlled by advection in bottom boundary layer. This plume can be classified as bottom-advected plume with small *S* and *Ro.*

The shore perpendicular source model may be compare with the Mississippi River and Atchafalaya River outflows. The shelf geometry determines the plume

characteristics when the buoyant inflow properties are same. For both rivers, the geometry is very different. Atchafalaya River has much wider estuary than the Mississippi River. The Atchafalaya river plume is not match the ideal model presented here, since it is a bottom-advected plume. However, the Mississippi River plume has many of the same characteristics as the idealized models previously presented.

During nonsummer season, Mississippi River flows to west (Li et al., 1997). In the summer season, however, the Mississippi river water cannot penetrate to the west, since the shifted winds push the river water to the east. In the summer season, however, the Mississippi river water cannot penetrate to the west, since the shifted winds push the river water to the east. A front west of the delta area and eventually, river water cannot penetrate further to the west at all.

It is expect that the frontal position representing the westward boundary of the plume will change in time, because alongshore penetration of buoyant currents is proportional to freshwater input and inversely proportional to upwelling wind stress strength, both of which change in time. Lots of river water discharge causes the river water to penetrate further to the west, but strong upcoast wind prevents river extension to the west and pushes the front to the east.

When strong wind blowing summer, fresh water pool is created in early stage in summer because strong wind can quickly prevents river water penetration by faster set up of the strong front near the estuary than weak wind.

Blocked river water creates fresh water pool in the east side of the Mississippi delta and extends to east along shore and offshore and mid Gulf of Mexico by mid scale anticyclonic eddy in Northern Gulf of Mexico (Morey et al., 2005).

CHAPTER V

CONCLUSION

During summer season, upcoast wind prohibits downcoast spreading of river water and made fresh water pool in the Texas-Louisiana shelf. To understand generation mechanism we studied the reaction of plume and resulting buoyancy driven current under the upwelling conditions with an ideal model, focusing on the penetration rate of fresh water downcoast under upwelling favorable wind conditions.

This study demonstrates that alongshore penetration of buoyant currents is proportional to freshwater input and inversely proportional to upwelling wind stress strength**.** Large freshwater inflow causes freshwater to penetrate further into the salty water, but strong upwelling wind counteracts this. Under the strongest wind conditions, used in this study, the fresh water cannot penetrate at all into ambient salty water. Strong wind quickly prevents fresh water's penetration, through a fast set up of a strong front near the estuary mouth.

The shore perpendicular source case front location is much closer to the estuary than shore parallel source case because as large portion of freshwater is stored in a bulge, causing the alongshore current freshwater transportation volume to be reduced. The shore parallel source case doses not have such a bulge.

The highest surface point of plume is a good proxy for determining the center of the plume. To find out the detachment rate of the bulge from the coast and its path, selecting the bulge center is important. The highest surface point of plume well matches

the bulge's middle point, and it is also reasonable based on a geostrophic balance of the flow around the bulge. Thus, the center of the anticyclonic bulge is defined as the highest sea surface height.

When the bulge detaches from the coast, it behaves like a slab, and moving upcoast and offshore with a 45 degree angle. Because the plume moves as an Ekman layer, without change of thickness, the bulge behaves like a slab. The mean flow, a coastal jet flowing upcoast, is driven by upwelling wind, and moves the bulge upcoast at it is simultaneously advected to the offshore by Ekman transport. These processes combine to move the bulge northeast with a 45 angle to the coast.

All tracks of the bulge follow the same path, despite different wind strengths. The path of the bulge is linear, and is independent of strength of wind.

Bulge moving speed has a linear relationship with the wind stress strength. As the wind stress increases, the bulge moving speed increases linearly. The simulated bulge moving speed well matches the expected speed. The simulated bulge moving speeds are calculated through the time rate of change of the distance from the estuary mouth to plume center. The expected moving speed is calculated by an equation based on Ekman transport, as the Ekman balance is the main component of the alongshore momentum balance.

The front and the plume movement are coherent and have an inverse relationship. As the wind stress increases, the plume advection speed increase linearly, but the alongshore fresh water penetration exponentially decreases.

The plume has an asymmetric response to upwelling and downwelling and fresh water flux is changed immediately by wind. So, alongshore transport may be modified

by order one under the wind stress.

During downwelling, the along-shore fresh water transport becomes greatest and during upwelling it is reduced. During upwelling, the plume detaches from the coast and along shore flow becomes weak. Background mean flow can substantially increases alongshore freshwater transport.

Mean flow can enhance or reduce the effects of upwelling and downwelling. For the duration of downwelling, a strong alongshore current is formed that enhances the response of the plume to the wind. However, during upwelling, the mean flow can reduce the effect of the wind effect by an upcoast flow. In the sinusoidal wind with mean flow case, the fresh water flux is higher value than the no mean flow sinusoidal wind case. This shows that means flow can enhance alongshore fresh water flux.

REFERENCES

Austin, J. A., and S. J. Lentz, 2002: The inner shelf response to wind-driven upwelling and downwelling. *J. Phys. Oceanogr.,* **32,** 2171-2193.

Berdeal, I. G., B.M. Hickey, and M. Kawase, 2002: Influence of wind stress and ambient flow on a high discharge river plume. *J. Geophys. Res.,* **107** (C9), 1330, doi:10.1029/200JC000932.

Brooks, D. A., 1994: A model study of the buoyancy-driven circulation in the Gulf of Maine. *J. Phys. Oceanogr.,* **24**, 2387-2412.

Chao, S., and W. C. Boicourt, 1986: Onset of estuarine plumes. *J. Phys. Oceanogr.,* **16**, 2137-2149.

Chao, S., 1988: River-forced estuarine plumes. *J. Phys. Oceanogr.,* **18,** 72-88.

Chapman, D. C., and S. J. Lentz, 1994: Trapping of a coastal density front by the bottom boundary layer. *J. Phys. Oceanogr.,* **24,** 1464-1479.

Cho, K., 1996: Three dimensional structure and variability of low-frequency currents on the Texas-Louisiana shelf based on moored current meter data. Ph.D. dissertation, Texas A&M University*,* 121pp

Cho, K., R. O. Reid, and W. D. Nowlin, Jr., 1998: Objectively mapped stream function fields on the Texas-Louisiana shelf based on 32 months of moored current meter data. *J. Geophys. Res.,* **103** (C5), 10**,**377-10,390.

Cochrane, J. D, and F. J. Kelly, 1986: Low-frequency circulation on the Texas-Louisiana continental shelf. *J. Geophys. Res*., **91** (C9), 10**,**645-10,659.

Dinnel, S. P. and W. J. Wiseman, Jr, 1986: Fresh water on the Louisiana and Texas shelf. *Continental Shelf Res.*, **6**, 765-784.

Dunn, D. D., 1996: Trends in nutrient inflows to the Gulf of Mexico from streams draining the conterminous United States 1972-1993. U.S. Geological Survey, water-resources investigations report 96-4113. Prepared in cooperation with the U.S. Environmental Protection Agency, Gulf of Mexico program, nutrient enrichment issue committee. Austin, TX: U.S. Department of the Interior, U.S. Geological Survey.

Flather, R. A., 1976: A tidal model of the northwest European continental shelf. *Memoires de la Societe Royale des Sciences de Liege* **6**, 10, 141-164.

Fong, D. A., W. R. Geyer, and R. P. Signell, 1997: The wind-forced response of a buoyant coastal current: Observations of the western Gulf of Main plume. *J. Mar. Syst.,*

12, 69-81.

Fong, D. A., and W. R. Geyer, 2001: Response of a river plume during an upwelling favorable wind event. J. *Geophys. Res.* **106** (C1), 1067-1084.

Garvine, R. W., 1987: Estuary plumes and fronts in shelf waters: A layer model. *J. Phys. Oceanogr.,* **17,** 1877-1896.

Garvine, R. W., 1995: A dynamical system for classifying buoyant coastal discharges. *Con. Shelf. Res.,* **15**, 1585-1995.

Garvine, R. W., 1999: Penetration of buoyant coastal discharge onto the continental shelf: A numerical model experiment. *J. Phys. Oceanogr***. 29**, 1892-1909.

Haidvogel, D. B., and A. Beckmann, 1999: *Numerical Ocean Circulation Modeling*. Imperial College Press.

Haidvogel, D. B., H. Arango, K. Hedstrom, A. Beckmann, P. Malanotte-Rizzoli, and A. Schepetkin, 2000: Model evaluation experiments in the North Atlantic basin: Simulations in nonlinear terrain-following coordinates. *Dyn. Atmos. Oceans* **32**, 239-281.

Hallock, Z. R., and G. O. Marmorino, 2002: Observations of the response of a buoyant estuarine plume to upwelling favorable winds. *J. Geophys. Res.,* **107** (C7), 3066, doi:10.1029/200JC000698.

Hetland, R. D., 2005: Relating river plume structure to vertical mixing. *J. Phys. Oceanogr.,* **35**, 1667-1688.

Hickey, B. M., L. J .Pietrafesa, D. A. Jay, and W. C. Boicourt, 1998: The Columbia River plume study: Subtidal variability in the velocity and salinity fields. *J. Geophys. Res.,* 103 (C5), **10**,339-10,368.

Horner-Devine, A. R., D. A. Fong, S. G. Monismith, and T. Maxworthy, 2006: Laboratory experiments simulating a coastal river inflow. *J. Fluid Mech,* (accepted).

Houghton, R. W., C. E. Tilburg, R. W. Garvine, and A. Fong, 2004: Delaware River plume response to a strong upwelling-favorable wind event. *Geophys. Res. Lett.,* **31.** L07302.

Johnson, D. R., A. Weidemann, R. Arnone, and C. D. Davis, 2001: Chesapeake Bay outflow plume and coastal upwelling events: Physical and optical properties. *J. Geophys. Res.,* **106** (C6), 11,613-11,622.

Johnson, D. R., J. Miller, and O. Schofield, 2003: Dynamics and optics of the Hudson River outflow plume. *J. Geophys. Res*., **108** (C10), 3323, doi:10.1029/200JC001485.

Kaurafalou, V. H., L. Oey, J. D. Wang, and T. N. Lee, 1996: The fate of river discharge on the continental shelf, 1, modeling the river plume and the inner shelf coastal current. *J. Geophys. Res.,* **101** (C2), 3415-3434.

Lentz, S. J., 2004: The response of buoyant coastal plumes to upwelling-favorable winds. *J. Phys. Oceanogr.,* **34**, 2458-2469.

Li, Y., W. D. Nowlin, Jr., and R. O. Reid, 1996: Spatial-scale analysis of hydrographic data over the Texas-Louisiana continental shelf. *J. Geophys. Res.,* **101** (C9), 20,595-20,605.

Li, Y., W. D. Nowlin, Jr., and R. O. Reid, 1997: Mean hydrographic field and their interannual variability over the Texas-Louisiana continental shelf in spring, summer, and fall. *J. Geophys. Res.,* **102** (C1), 1027-1049.

Marchesiello, P., J. C. McWilliams, and A. Shechepetkin, 2001: Open boundary conditions for long-term integration of regional oceanic models. *Ocean Modelling.,* **3,** 1-20.

Mellor, G. L., and T. Yamada, 1982: Development of a turbulence closure model for geophysical fluid problems. *Rev. Geophys. Space Phys.,* **20,** 851-875.

Morey, S. L., J. Zavala-Hidalgo, and J.J. O'Brien, 2005: The seasonal variability of continental shelf circulation in the northern and western Gulf of Mexico from a high-resolution numerical model, in New Developments in the Circulation of the Gulf of Mexico, *Geophys. Mongr. Ser.161,* edited by W. Sturges and A. Lugo-Fernandez, AGU, Washington, D.C.

Munchow, A., and R. W. Garvine, 1993: Dynamical properties of a buoyancy-driven coastal current. *J. Geophys. Res.* **98** (C11), 20,063-20,077.

Oey, L.-Y., and G. L. Mellor, 1993: Subtidal variability of estuarine outflow, plume, and coastal current: A model study. *J. Phys. Oceanogr*. **23**, 164-171.

Palma, E. D., Matano, R.P., 1998. On the implementation of passive open boundary conditions for a general circulation model: The barotropic mode. *J. Geophys. Res.,* **103** (C11), 1319-1341.

Rabalais, N. N., W. J. Wiseman, Jr., R. E. Turner, B. K. Gupta, Q. Dortch (1996). Nutrient changes in the Mississippi river and system responses on the adjacent continental shelf. *Estuaries,* **19**, 386-407

Rennie, S., J. T. Largier, and S. J. Lentz, 1999: Observations of low salinity coastal current pluses downstream of Chesapeake Bay. *J. Geophys. Res.,* **104,** 18,227-18,240.

Sanders, T. M., and R. W. Garvine, 2001: Fresh water delivery to the continental shelf and subsequent mixing: An observational study. *J. Geophys. Res.* **106** (C11), 27,087-

27,101.

Song, Y. and D. B. Haidvogel, 1994: A semi-implicit ocean circulation model using a generalized topography-following coordinate system. *J. Comp. Phys.*, **115,** *228-244.*

Wang, W., 1996: Analysis of surface meteorological fields over the northwestern Gulf of Mexico and wind effects on the circulation over the LATEX shelf. *Ph.D. dissertation, Texas A&M University,* 122pp.

Whitehead, J. A. and D. C. Chapman, 1986: Laboratory observations of a fresh water gravity current on a shelf: The generation of shelf waves. *J. Fluid Mech.*, **172**, 373-399.

Whitney, M. M., and R. W. Garvine, 2005:Wind influence on a coastal buoyant outflow. *J. Geophys. Res.* **110** (C3), C03014, doi:10.1029/2003JC002261.

Wiseman, W. J., Jr., J. M. Bane, S. P. Murray, and M. W. Tubman, 1976: Small-scale temperature and salinity structure over the inner shelf west of the Mississippi River Delta. *Men. Soc. R. Sci. Liege*, **6**, 277-285.

Wiseman, W. J., and S. P. Dinnel, 1988: Shelf currents near the mouth of the Mississippi River. *J. Phys. Oceanogr.,* **18**, 1287-1291.

Xing, J., and A. M. Davies, 1999: The effect of wind direction and mixing upon the spreading of a buoyant plume in a non-tidal regime. *Cont. Self Res.,* **19**, 1437-1483.

Yankovsky, A. E., and D. C. Chapman, 1997: A simple theory for the fate of buoyant coastal discharges. *J. Phys. Oceanogr.*, **27**, 1386-1401.

APPENDIX A

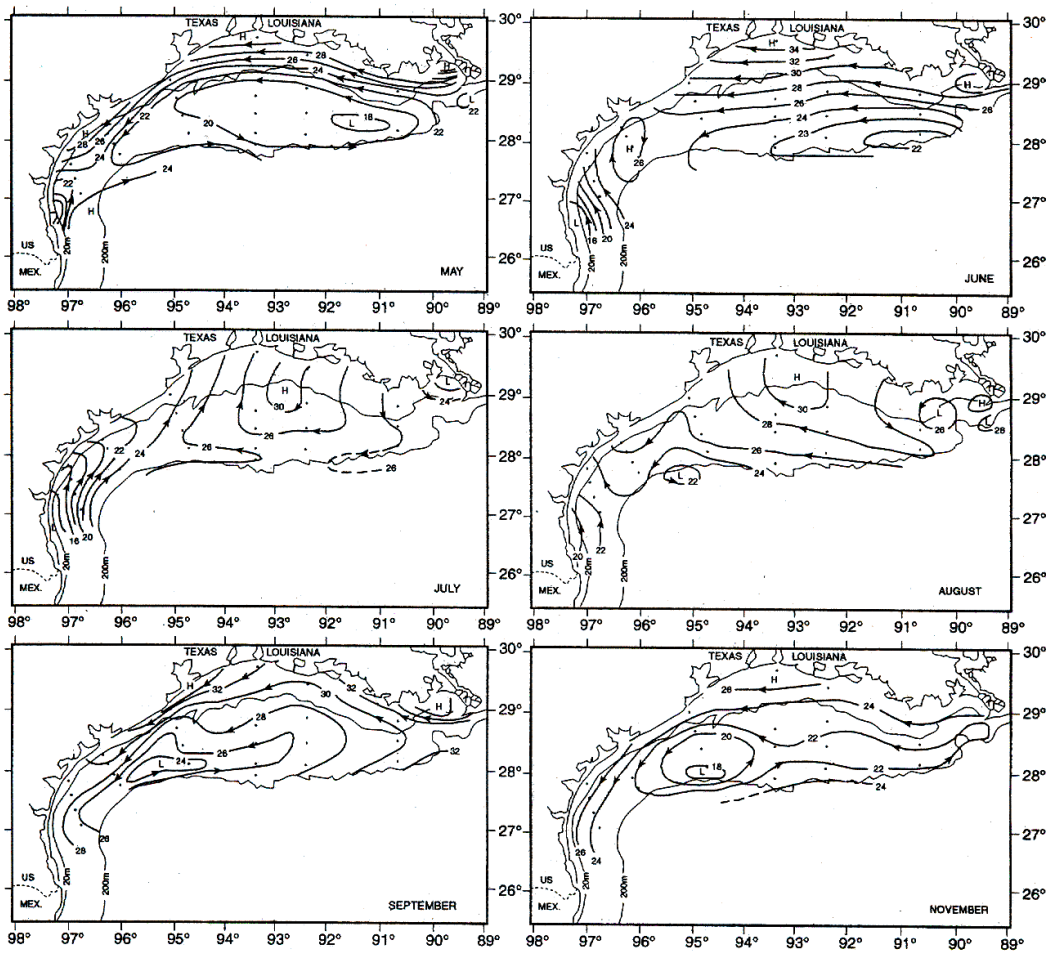

Figure 1. Monthly mean fields of surface geopotential anomaly. (Cochrane and Kelly, 1986). It suggests the general annual circulation pattern of the Texas-Louisiana shelf current.

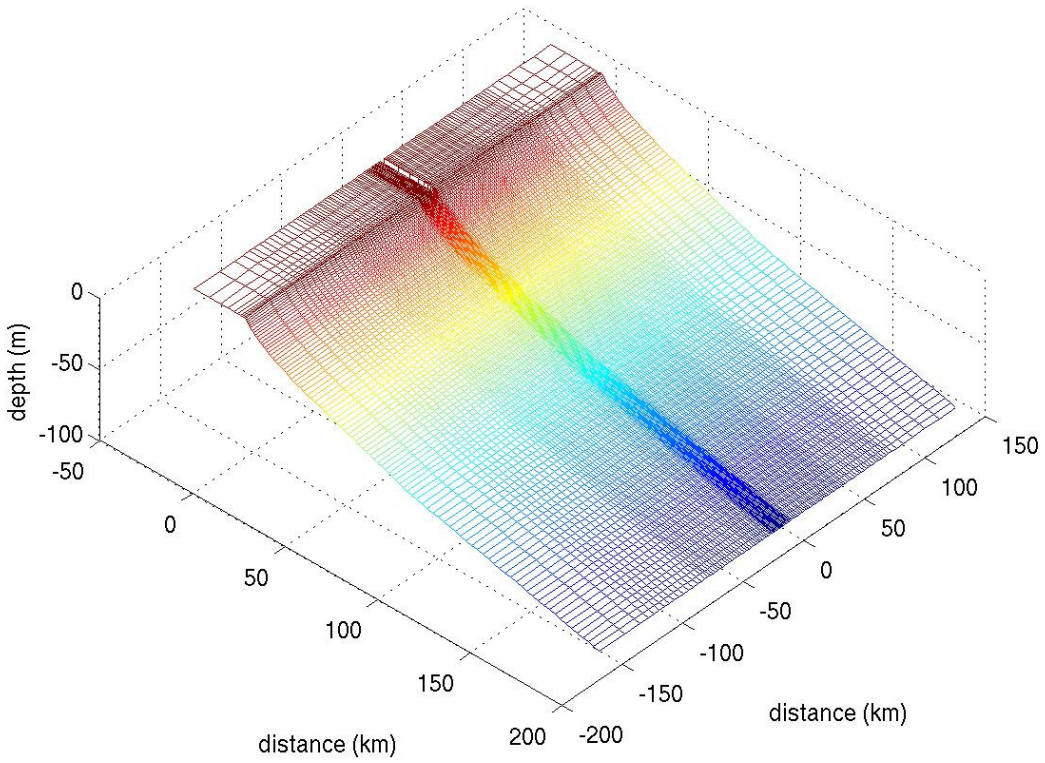

(a)

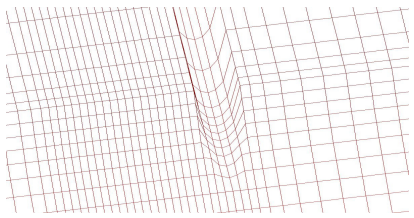

(b)

Figure 2. Plume model bottom topography. Rounded cross-channel estuarine is cut in through the shelf bathymetry has 1/2000 decline gentle slop. High resolution is specified alongshore coast and near the estuarine river water outflow region.

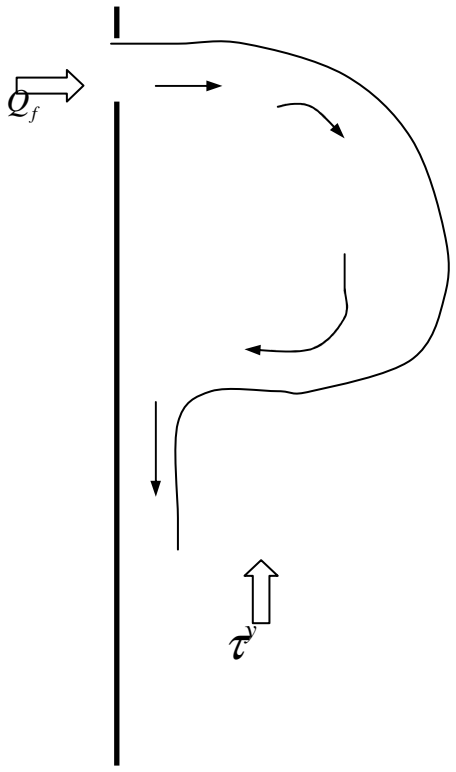

Figure 3. Schematic of a shore perpendicular source model.

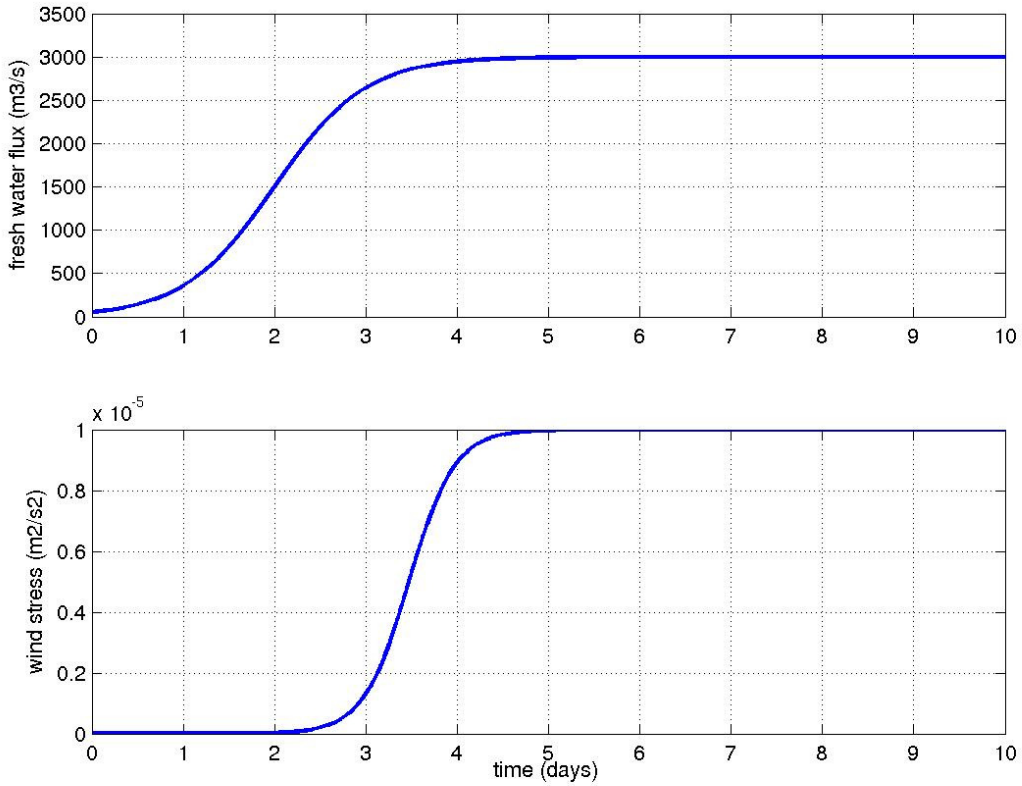

Figure 4. Model forcing. Fresh water flux(Q) and wind stress (τ/ρ_o), are applied by ramp with time-scale to prevent sudden forcing in the domain. Because it cause generate high frequency oscillations. Fresh water ramping time scale is 4 day and wind stress is 3 day.

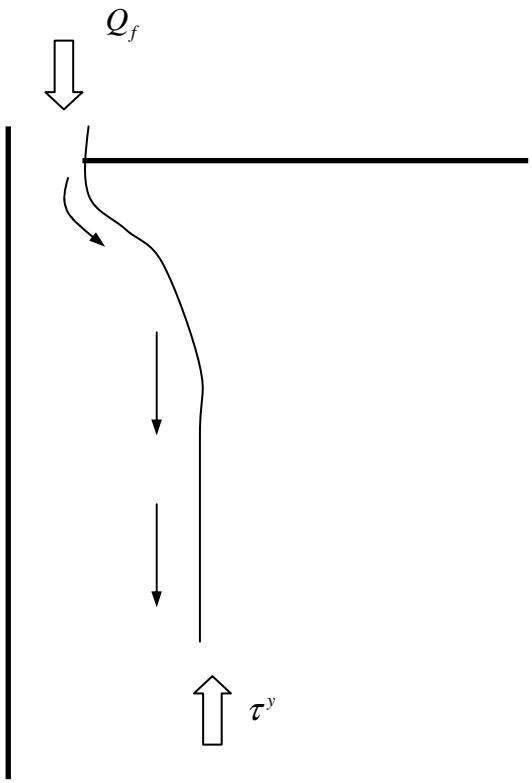

Figure 5. Schematic of shore parallel source model.

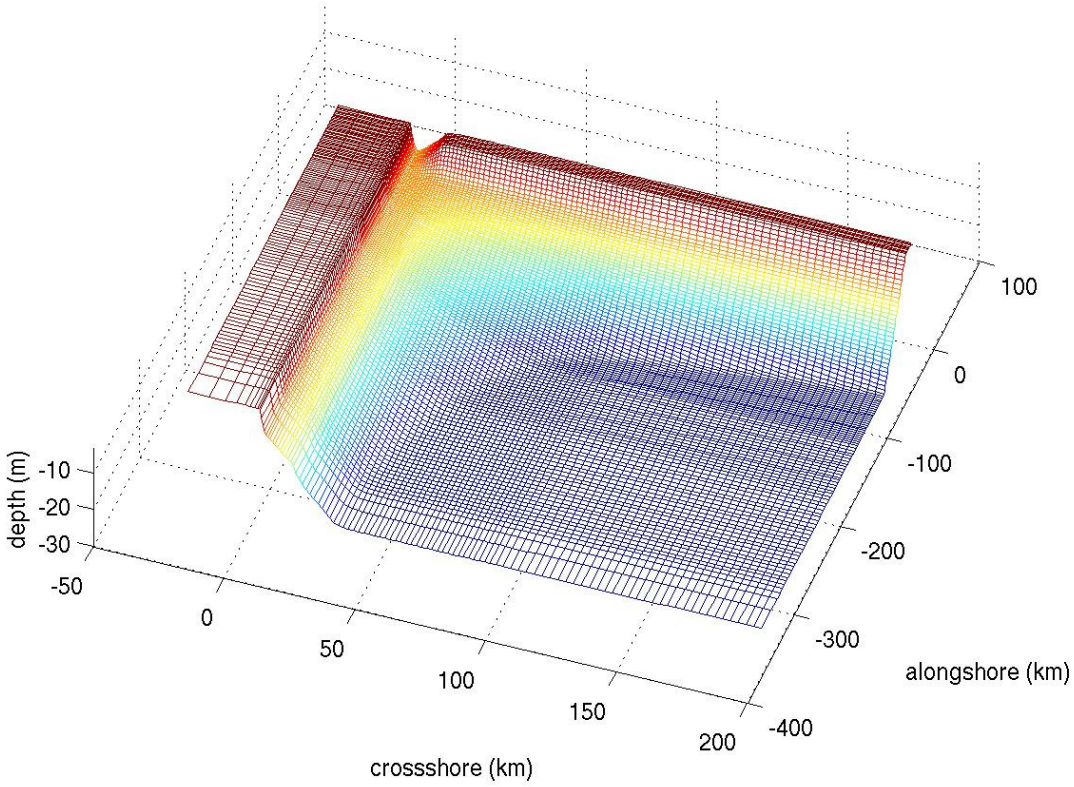

(a)

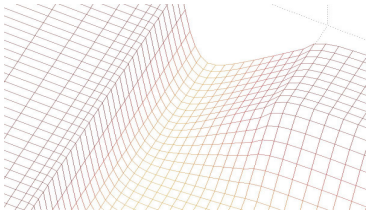

(b)

Figure 6. Shore parallel source model bottom topography. North wall and East wall connected 1/2000 gentle slop. Rounded cross-channel estuarine located in North wall. Maximum depth is limited as 30m. Higher resolution is specified alongshore coast and near the estuarine river water outflow region.

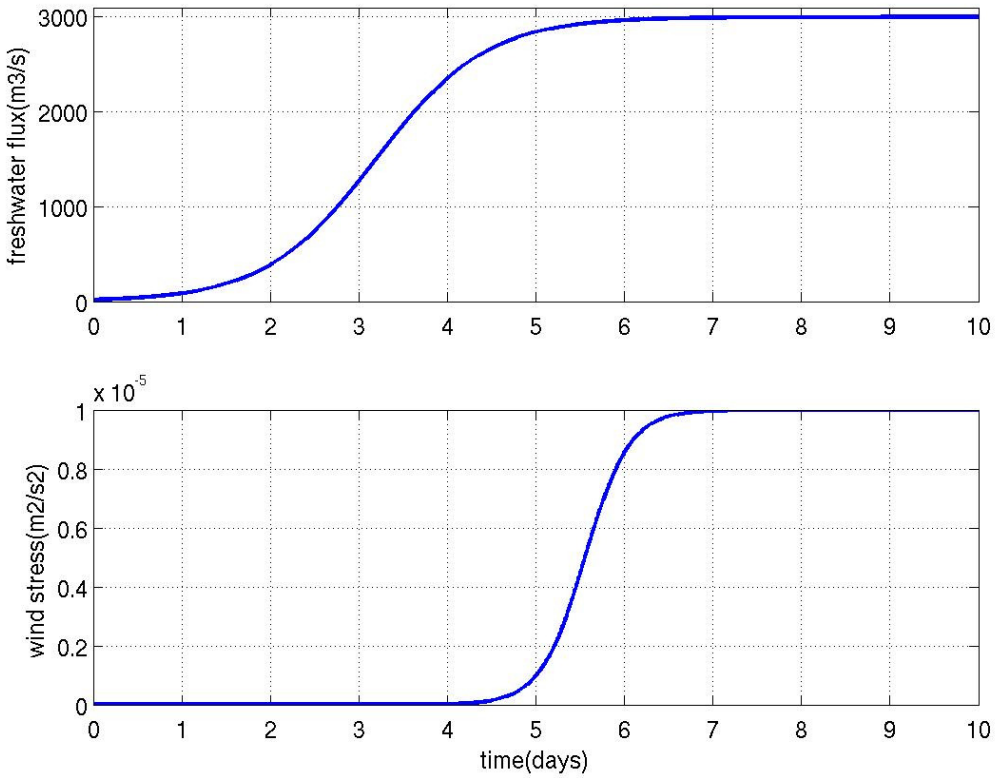

Figure 7. Model forcing. Fresh water flux(Q) and wind stress(τ / ρ_o), are applied by ramp with time-scale to prevent sudden forcing in the domain. Because it cause generate high frequency oscillations. Fresh water flux ramping time scale is 6 day and wind stress is 3 day.

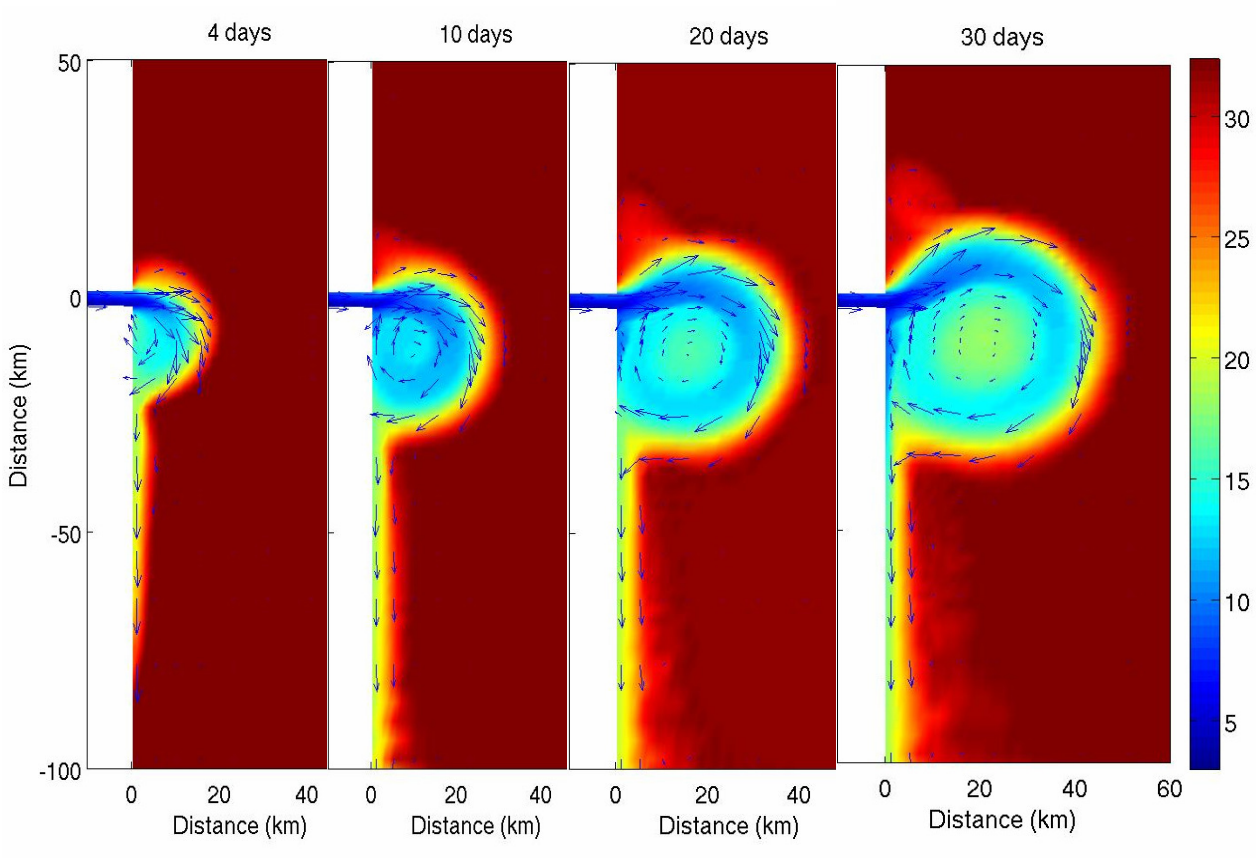

Figure 8. 4 time step figures of no wind forcing case. 4 time step figures show variation of plume in time under no extraordinary forcing. Fresh water turns anticyclonic and flow to south.

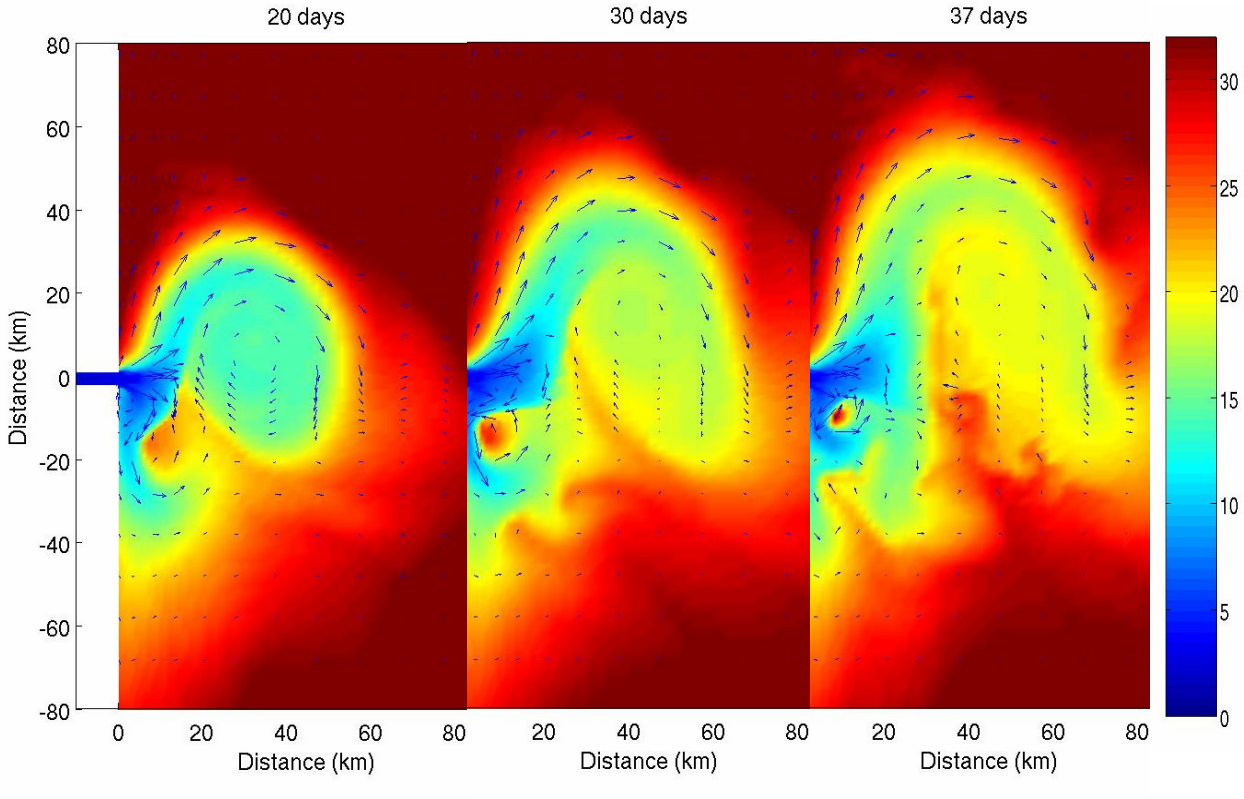

Figure 9. Upwelling wind case 3 time step bulge figures. Inflow is separated as two parts and supply to different bulge. One to original bulge and the other to second bulge newly formed. Small cyclonic rotation is formed by alongshore current returning flow in time.

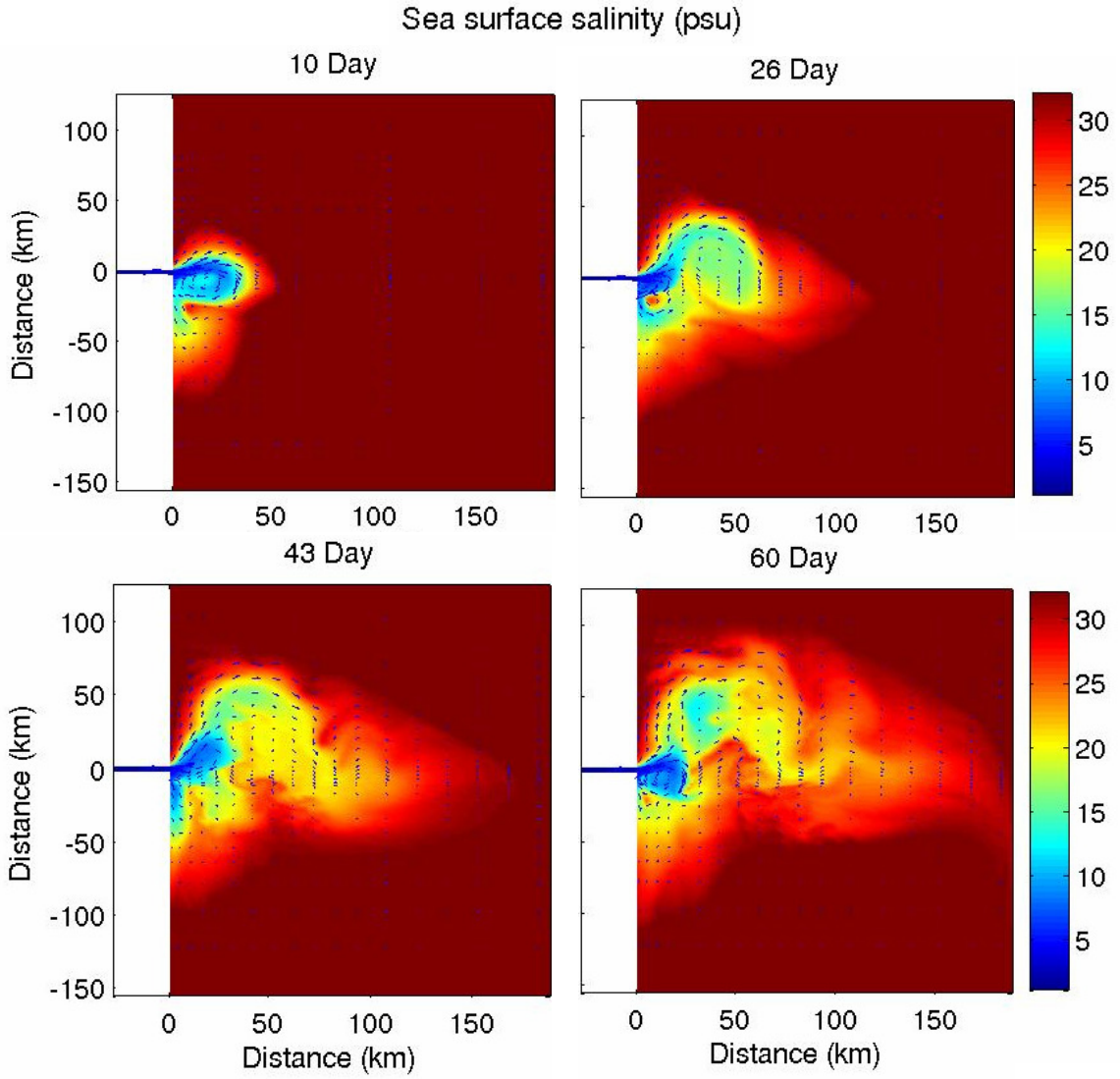

Figure 10. 4 time step figures of upcoast wind case. 4 time step figures show variation of plume in time pass under the upwelling favorable wind. It becomes unstable after formed new bulge and cyclonic rotation flow, 26 day figure showing, and dissipates at 60 day.

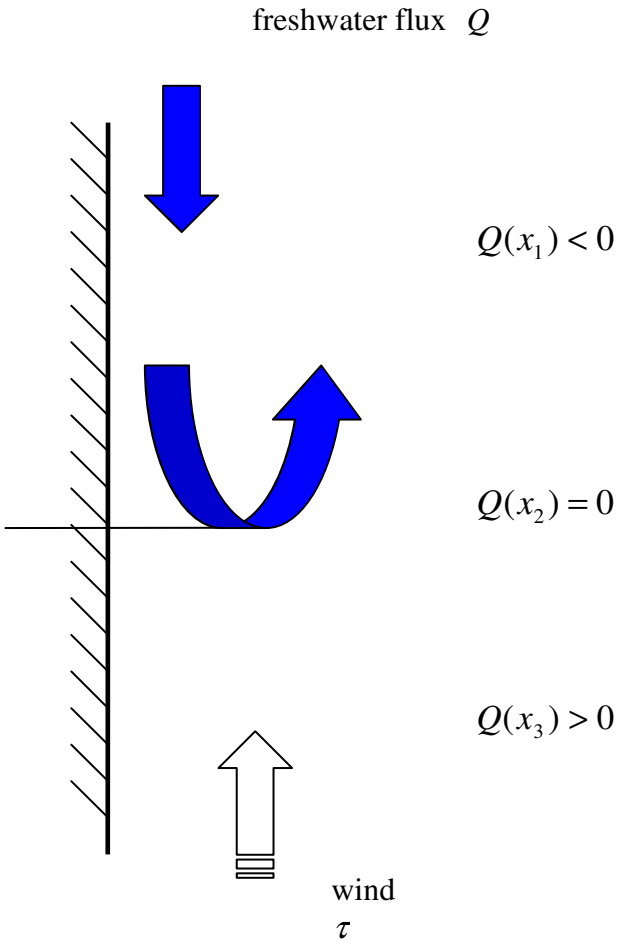

Figure 11. Schematic of alongshore south freshwater flux.

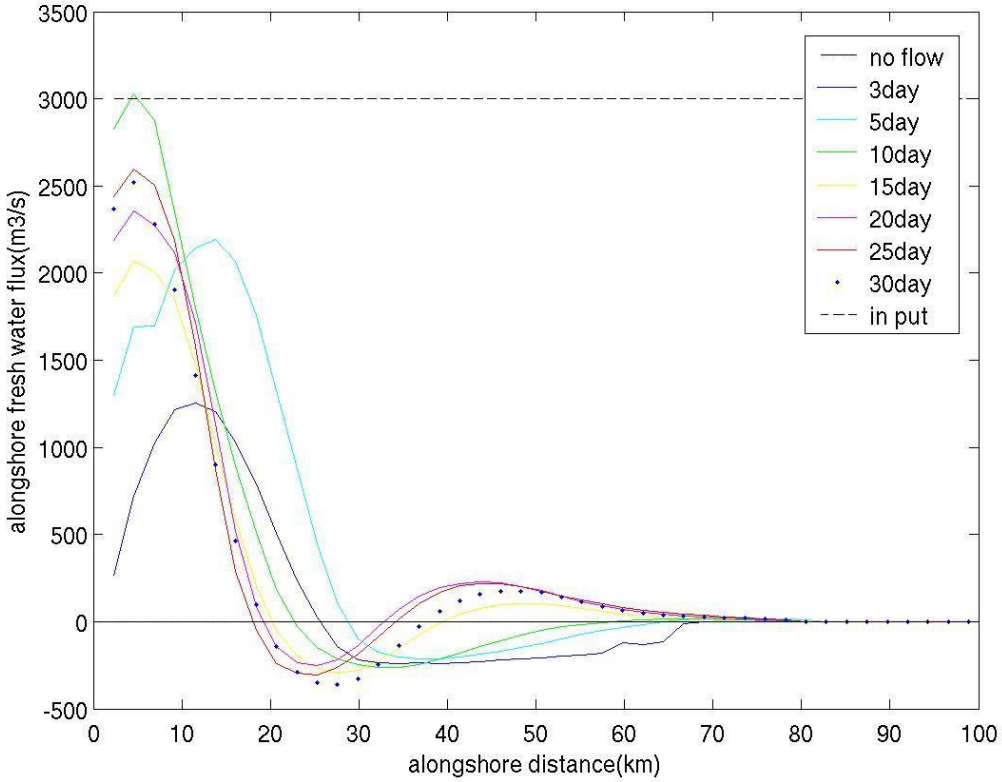

Figure 12. Fresh water flux variation. Front, flux zero point, is move northward in time. Fresh water flux Q = 3000 m^3 / s and wind stress $\tau / \rho_o = 0.1 m^2 / s^2$.

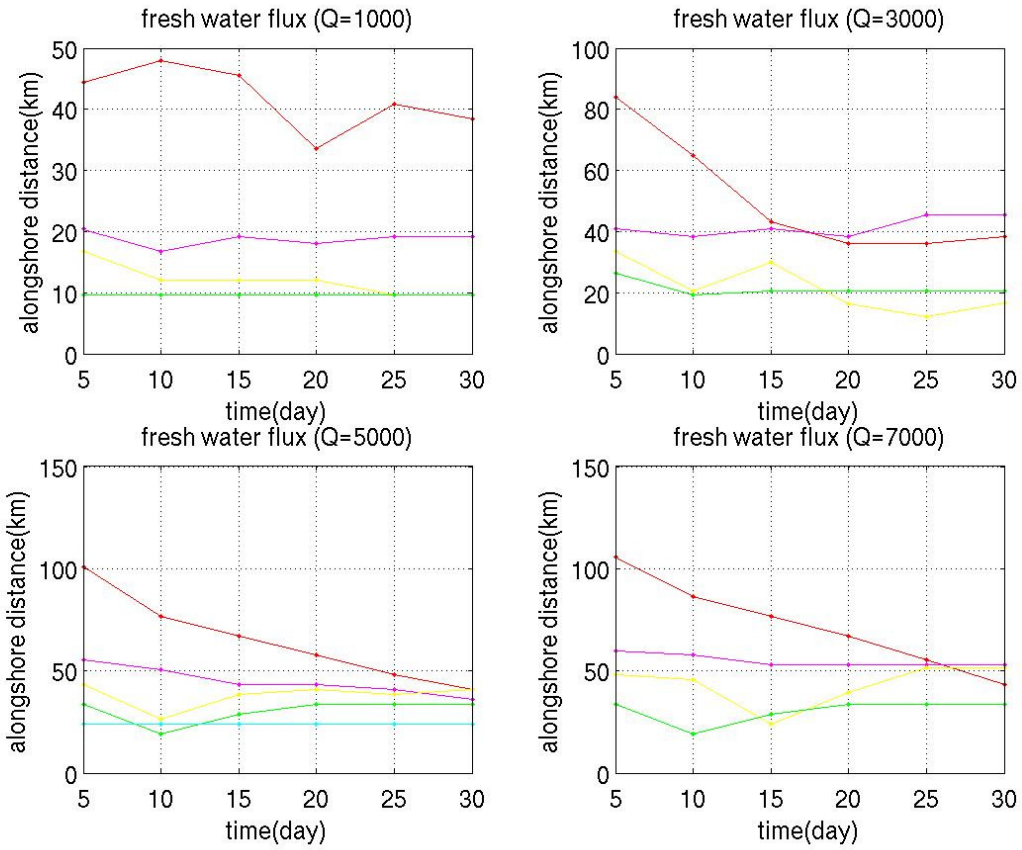

Figure 13. Front moving speed. It is based on wind stress and fresh water input flux. A strong wind more quickly prevents fresh water penetration by a faster set up of the front than a weak wind.
red – 0.1×10^{-4} m^2 s^{-2}
maroon-0.2×10^{-4} m^2 s^{-2}
yellow-0.3×10^{-4} m^2 s^{-2}
green-0.4×10^{-4} m^2 s^{-2}

Table 1. Front moving speed

	flux (m^3/s)			
$\tau/\rho_o(10^{-4}m^2/s^2)$	Q:1000	Q:3000	Q:5000	Q:7000
0.1	-1.7414	-8.7771	-10.843	-11.369
0.2	0	1.1829	-3.4171	-1.38
0.3	-1.1829	-3.3646	0.7229	1.4129
0.4	0	-0.7229	-3.0229	1.3143
0.5			0	1.7829

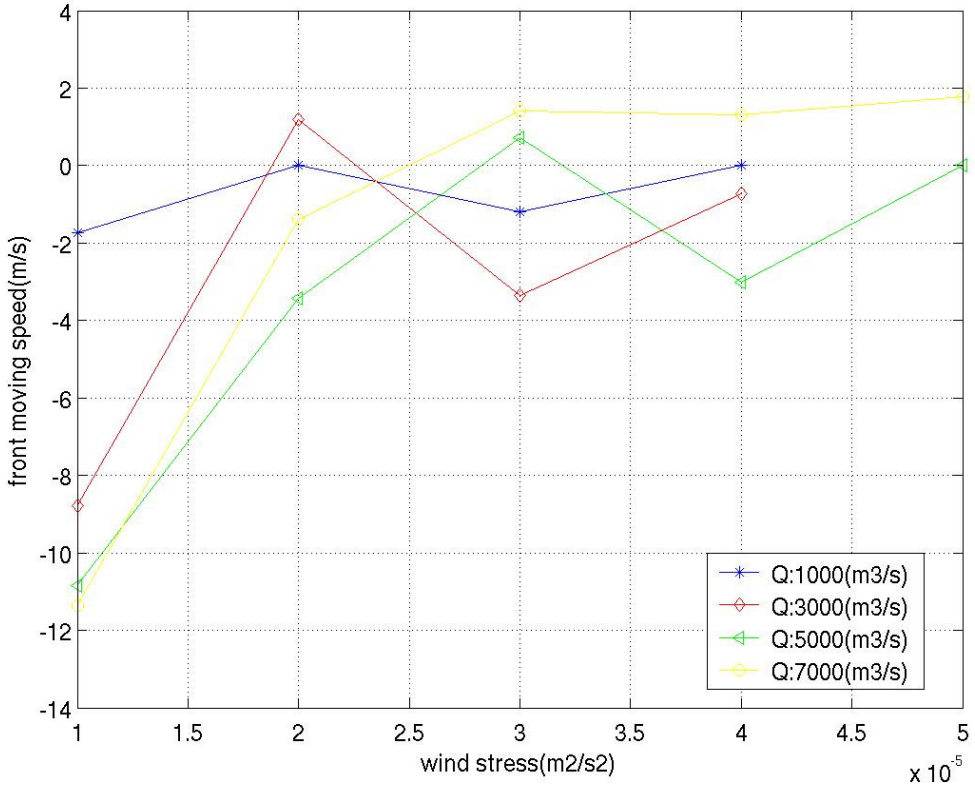

Figure 14. Front moving speed vs wind stress. A front moving speed exponentially decreases by the increase of wind stress.

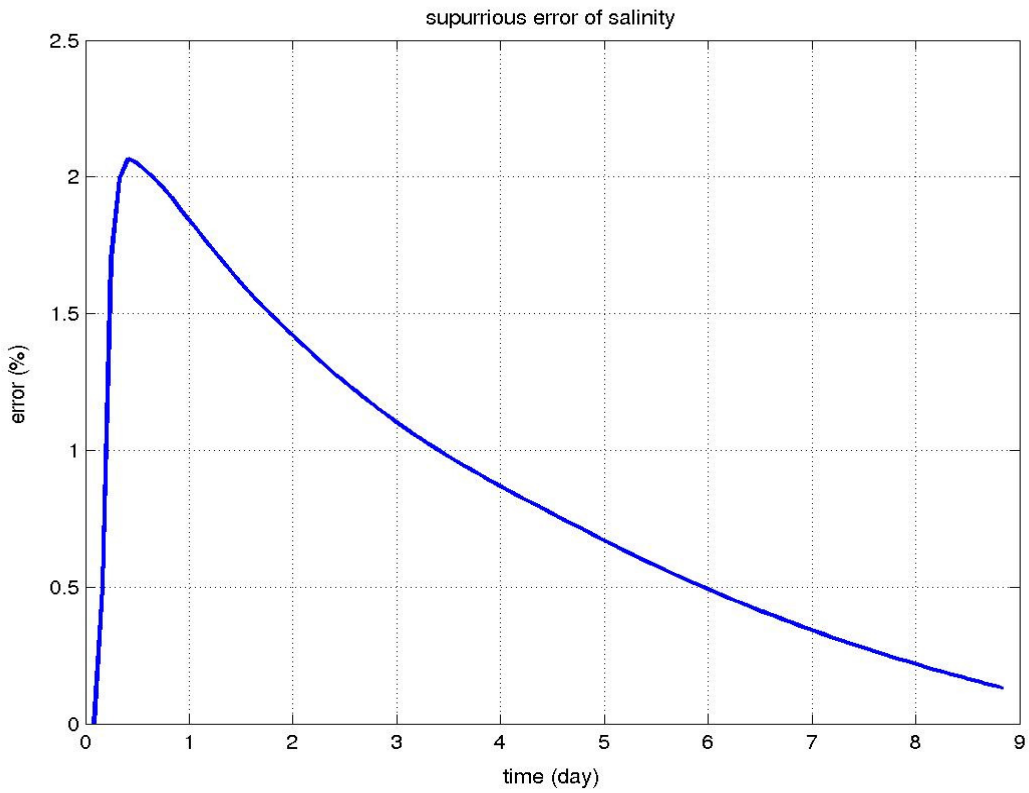

Figure 15. Spurious error. Longer ramping time scale generates smaller spurious error.

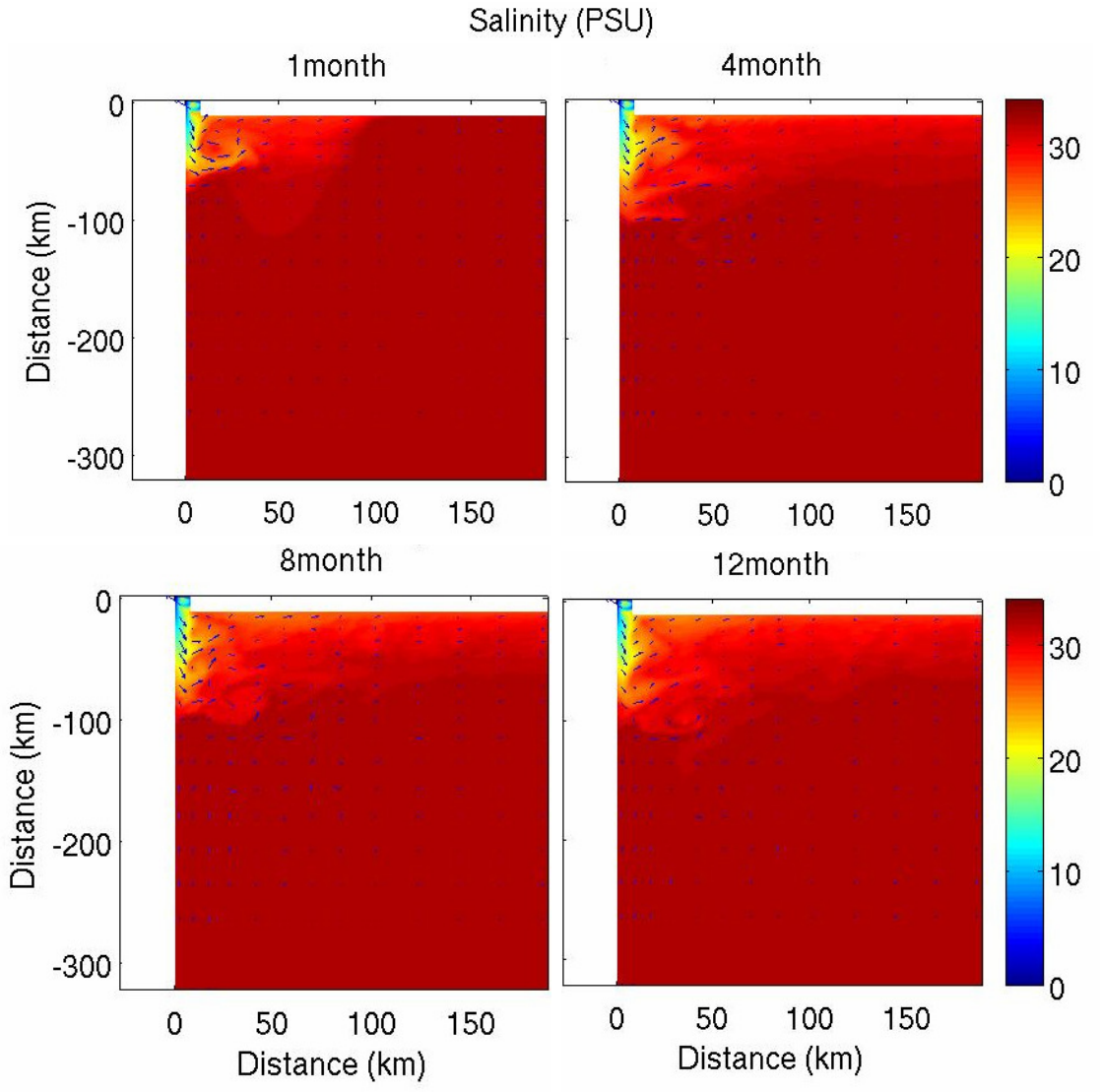

Figure 16. 4 time step figures of shore parallel source. 4 time step figures show stable front during 12 months.

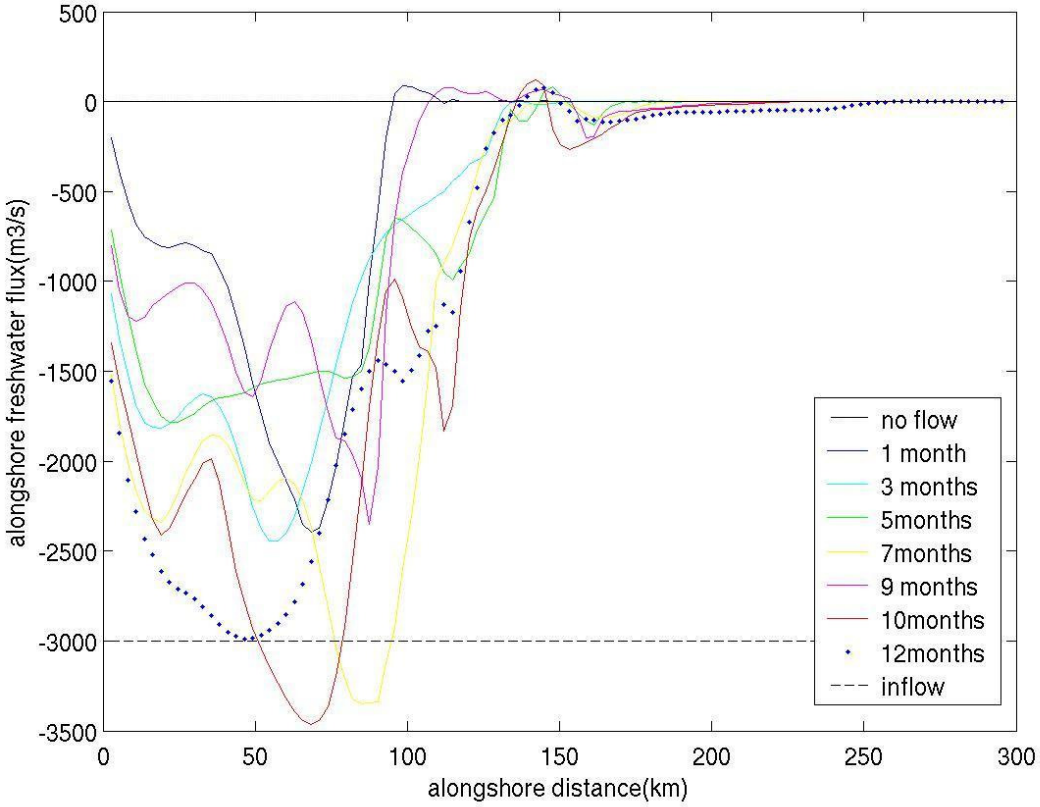

Figure 17. Fresh water flux variation. Front, flux zero point, is move northward as time pass. Fresh water flux Q = 3000 m^3 / s and wind stress $\tau / \rho_o = 0.1 m^2 / s^2$.

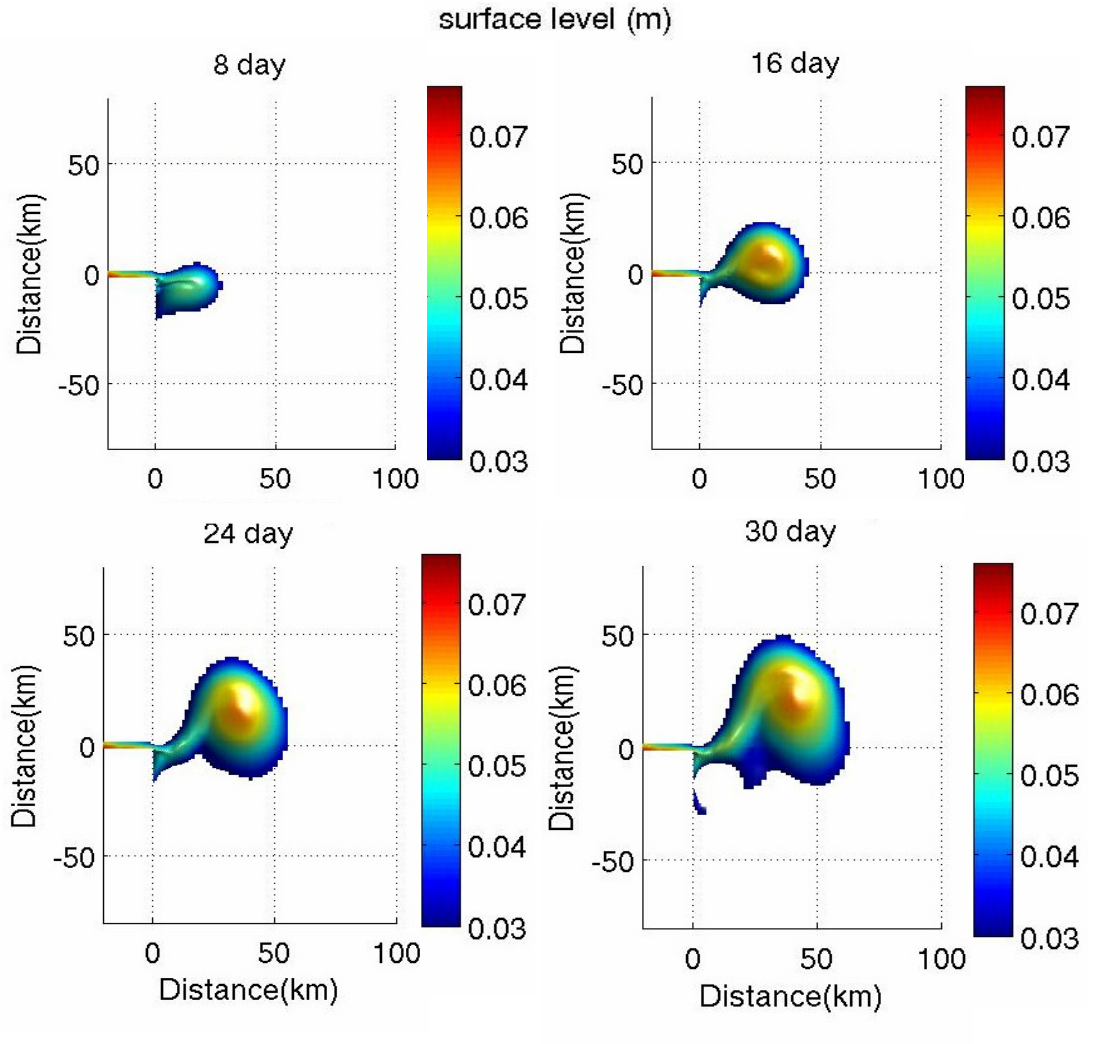

Figure 18. 4 time step figures of plume center. 4 time steps of plume movement figures for 1month. 45 degree northeast moving pattern is clearly presented by center of bulge path.

Table 2. Moving speed

Inflow Q: 5000 (m^3/s)			
τ/ρ_o	slope	mean error	time range (day)
0.1	1.0608	0.322	40
0.2	0.80147	0.003	20
0.3	1.068	0.001	16
0.4	0.71315	0.2795	12
0.5	0.9502	0.0003	10

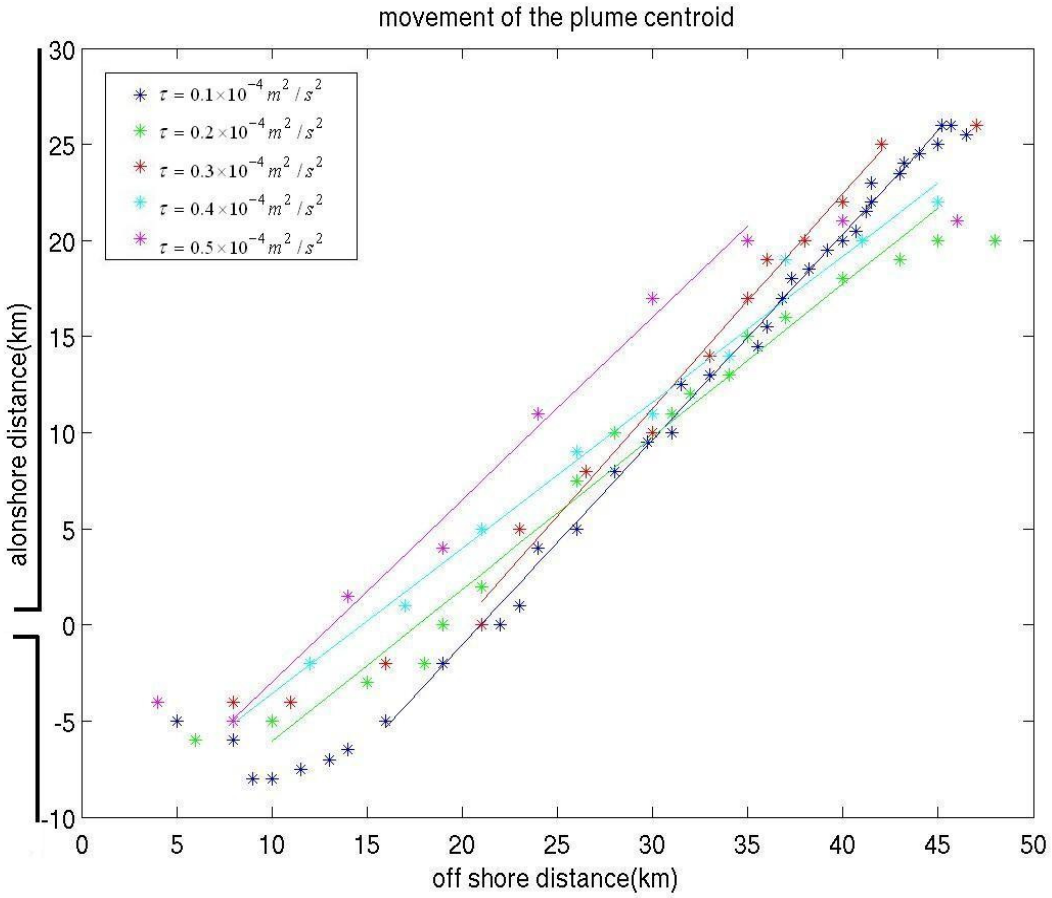

Figure 19. Movement of plume centroid. Points presented bulge center's daily position and fitted line show moving pattern.

Table 3. Compare speed

Inflow Q: 5000(m^3/s)		
τ/ρ_o	Simulated speed	Expected speed
0.1	1.294	1.44
0.2	2.4896	2.496
0.3	3.3965	3.3035
0.4	4.5912	4.4047
0.5	5.9066	5.3227

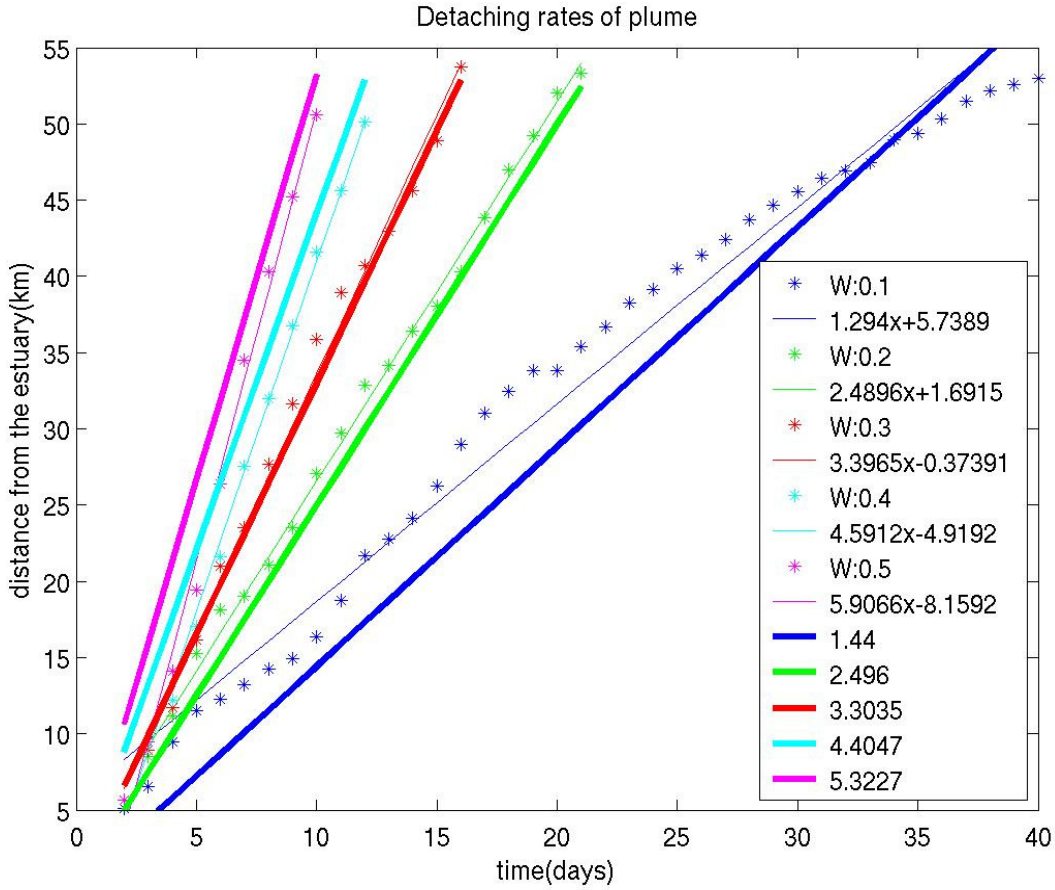

Figure 20. Simulated detaching speed (thin fitted line) vs. Ekman transport speed (thick line).

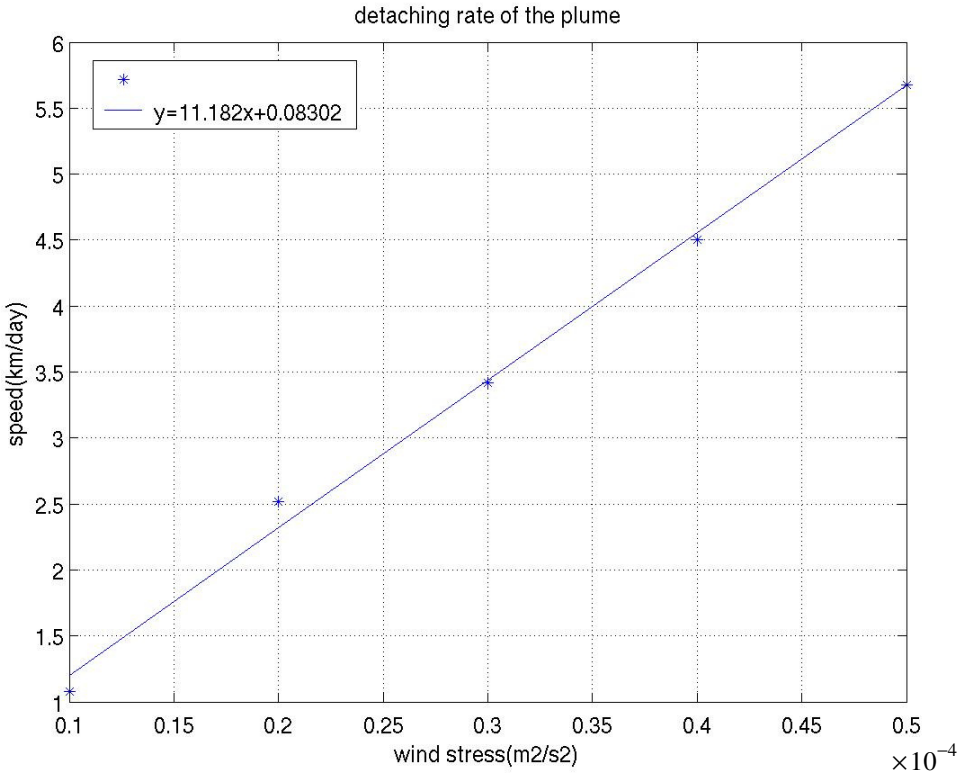

Figure 21. Plume moving speed vs. wind stress.

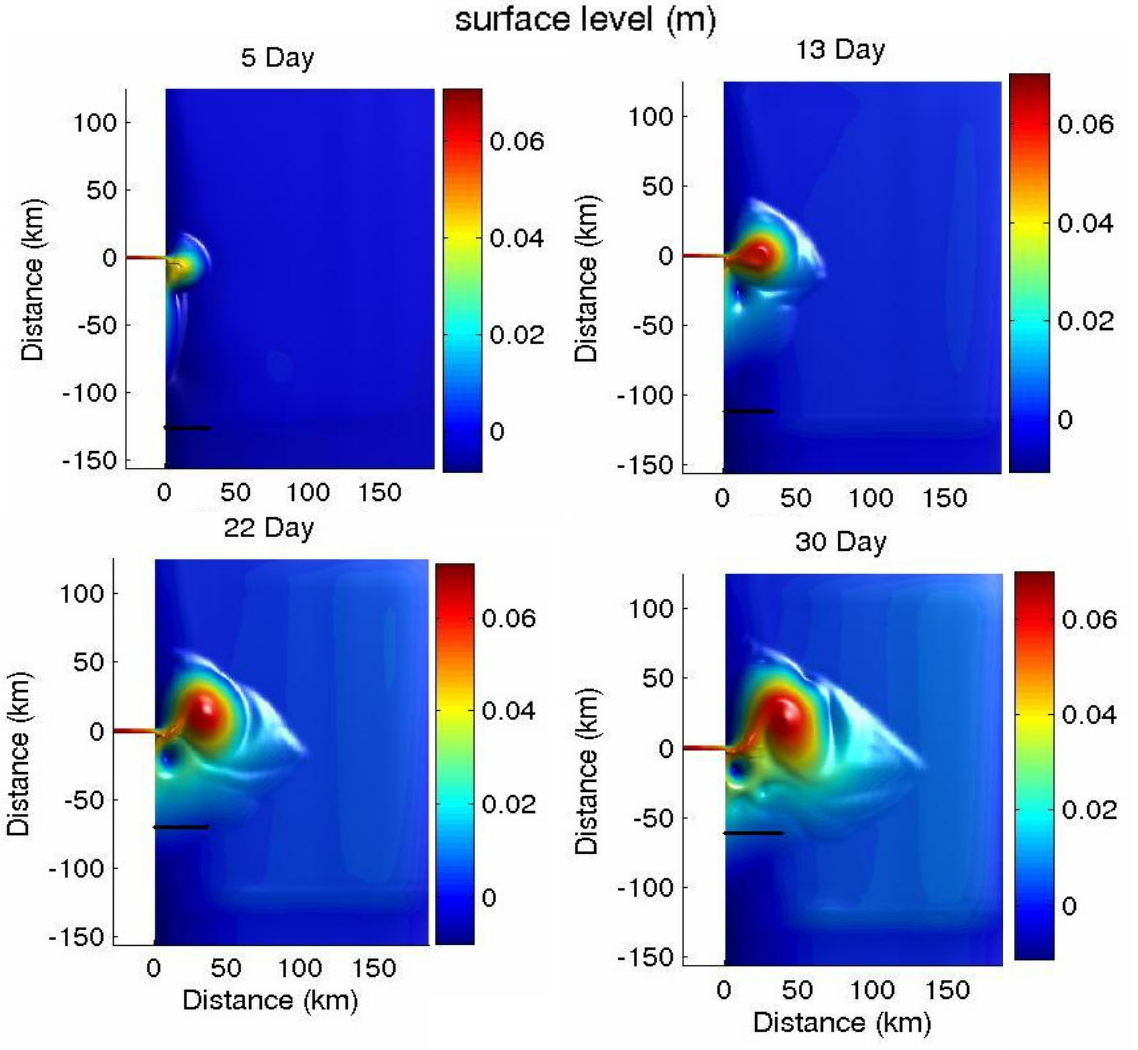

Figure 22. 4 time step figures plume & front. 4 time step figures show surface level during 1 month. Black line present front, flux () is 0. As highest surface, the plume center, advected to offshore front move to the north and approached estuary. Detachment rate of plume coherent with alongshore front movement.

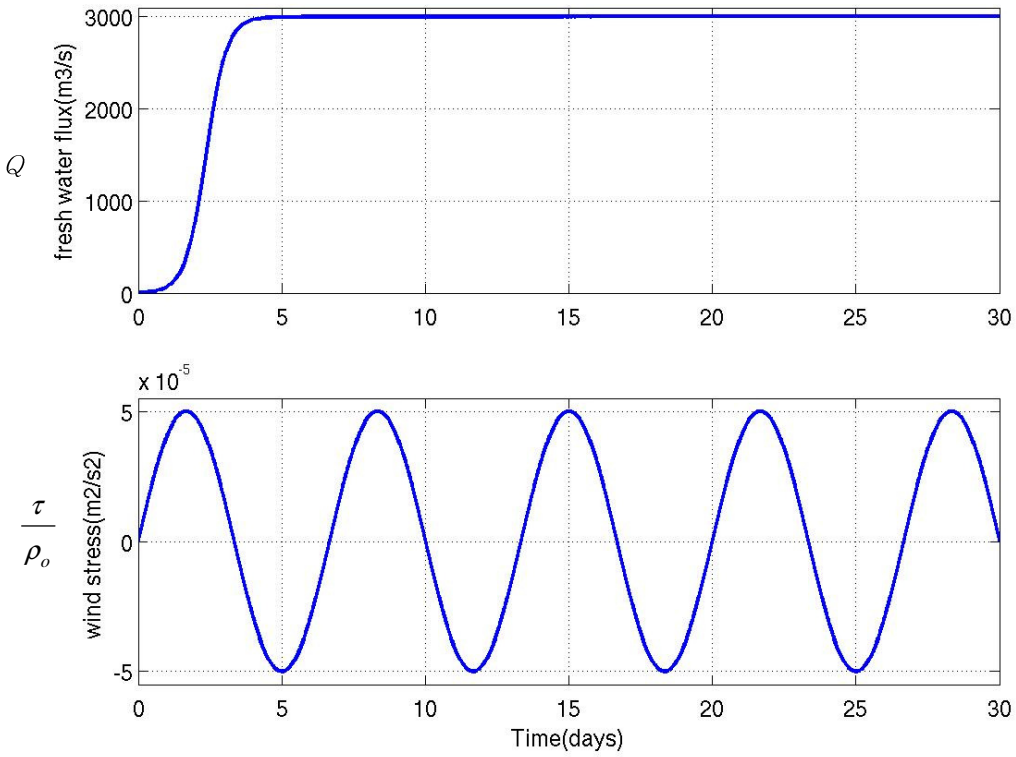

Figure 23. Forcing included sinusoidal wind. Fresh water flux ramping time scale is 4 day and wind period is 6.7 days.

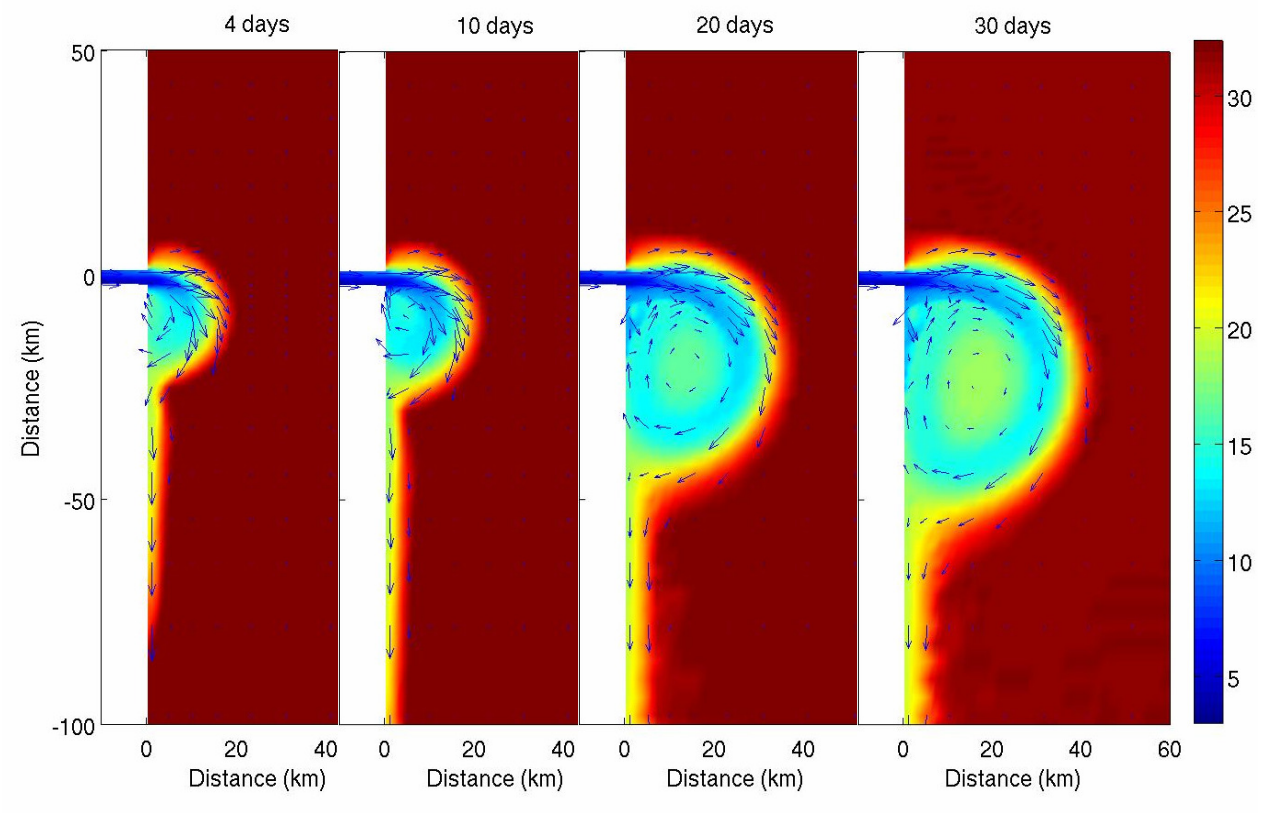

Figure 24. 4 time step figures of mean flow added case.

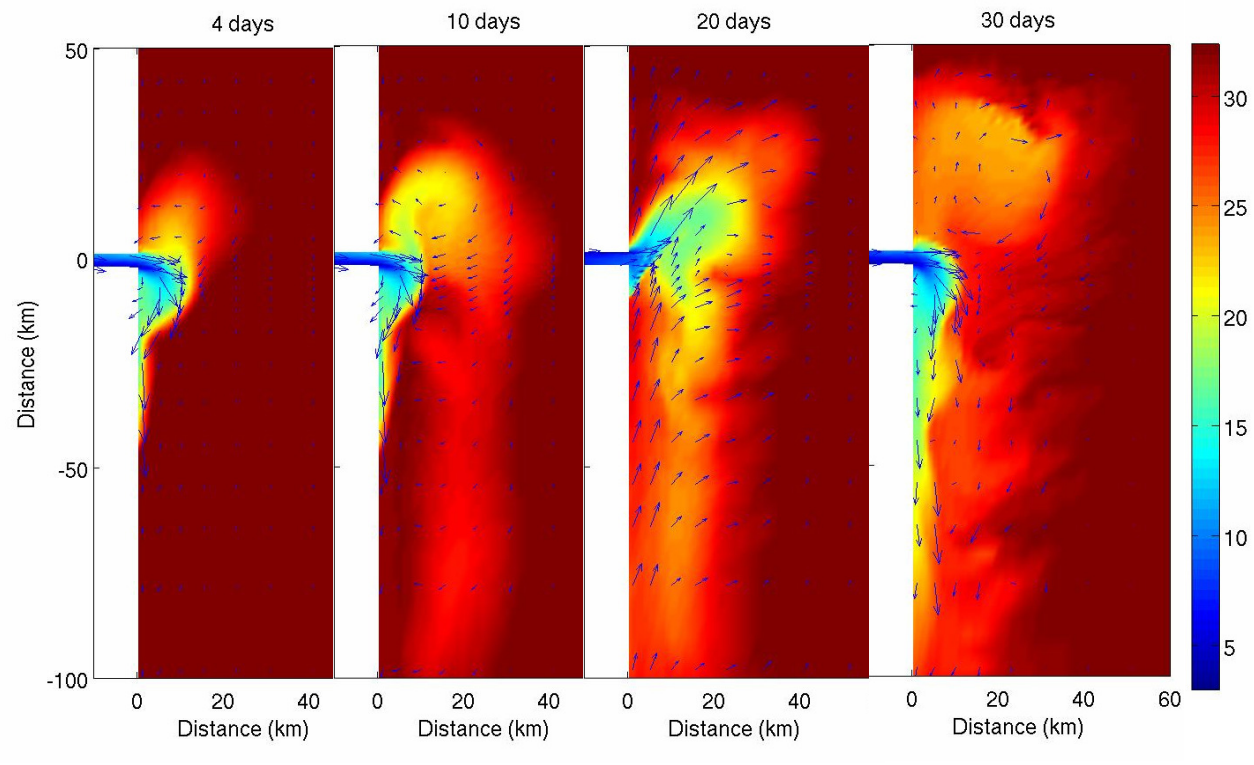

Figure 25. 4 time step figures of sinusoidal wind case.

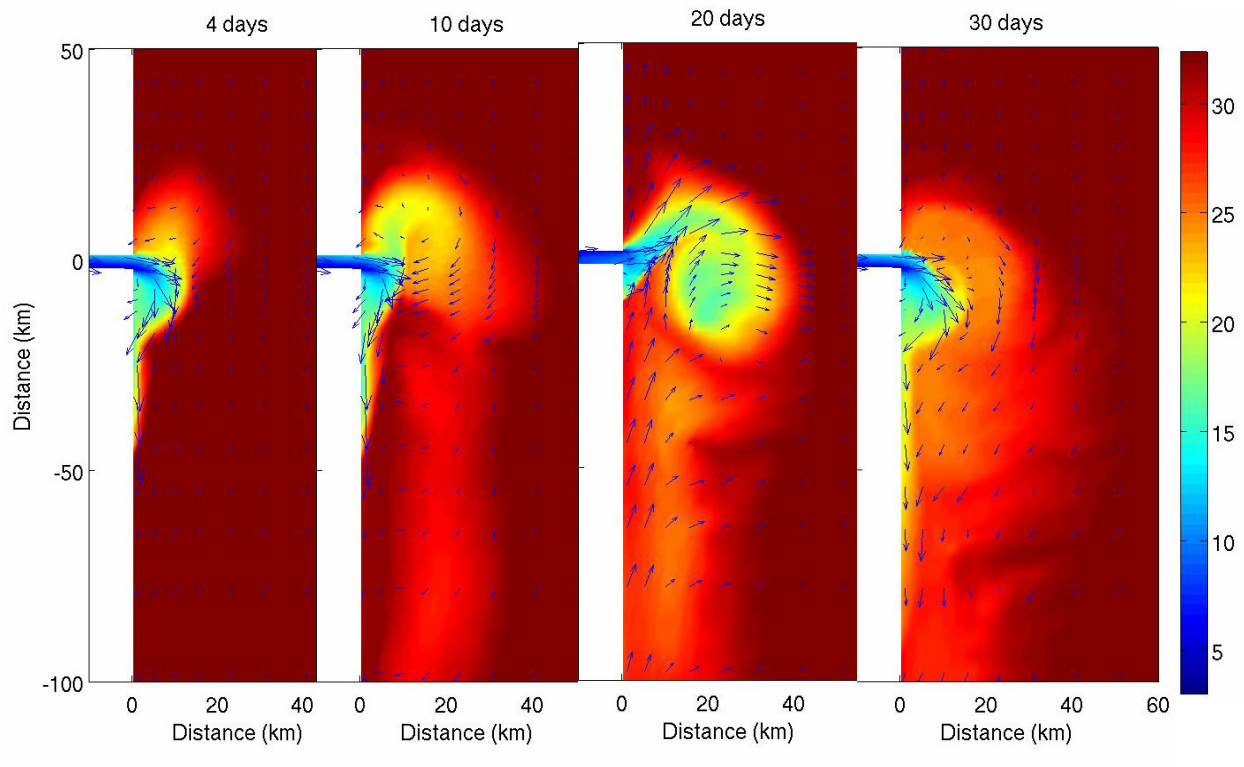

Figure 26. 4 time step figures of sinusoidal wind with mean flow.

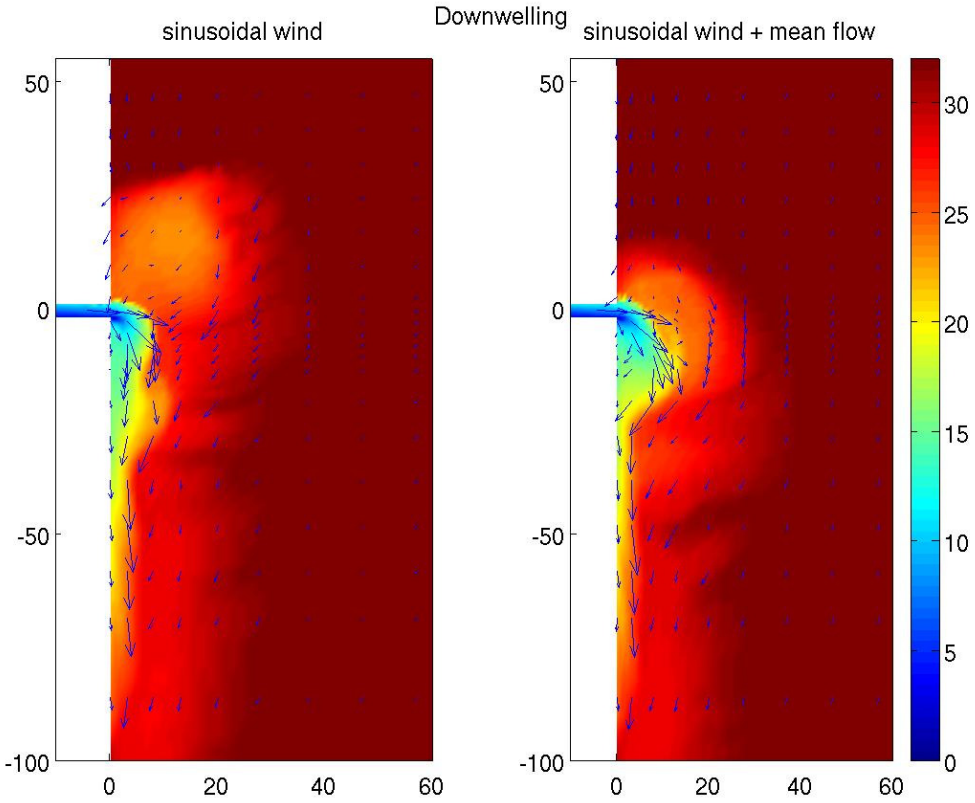

Figure 27. Downwelling of wind and wind with mean flow.

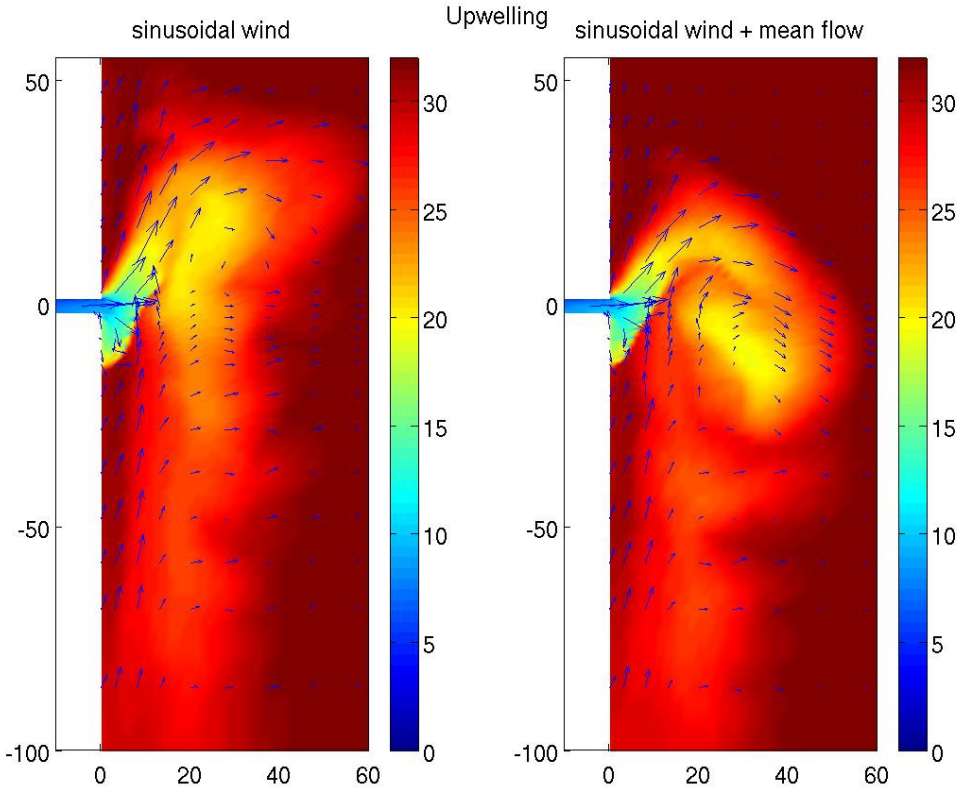

Figure 28. Upwelling of wind and wind with mean flow.

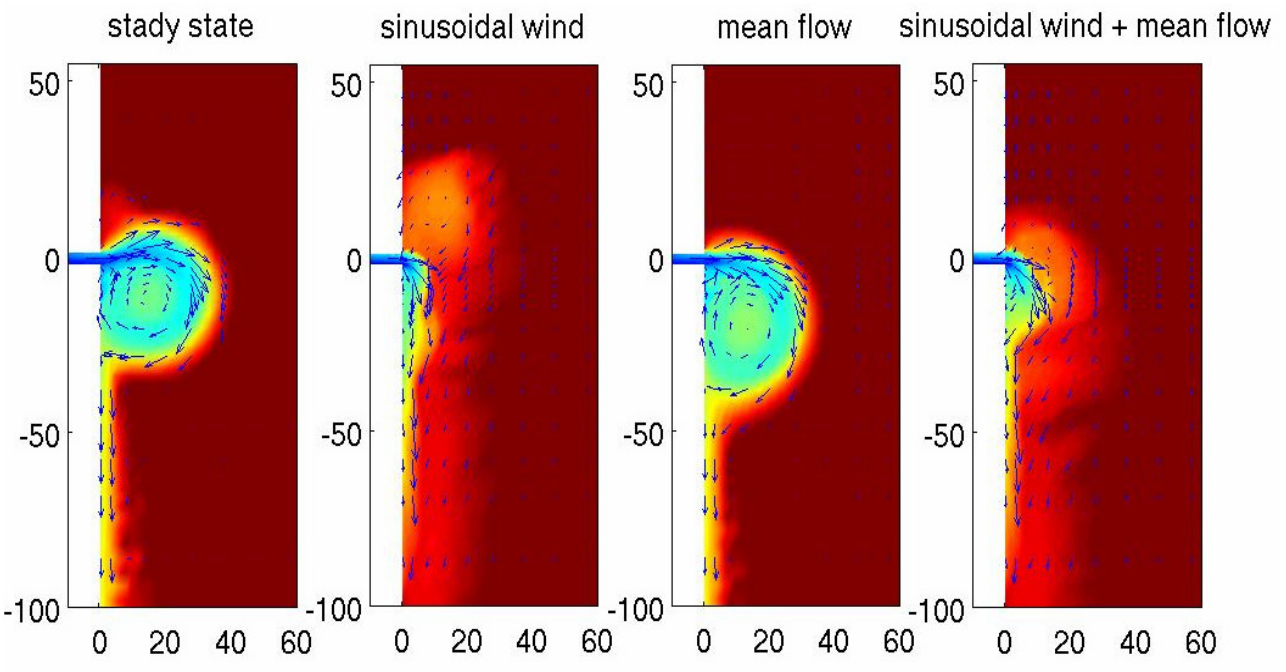

Figure 29. 4 time step figures of 4 difference case during downwelling.

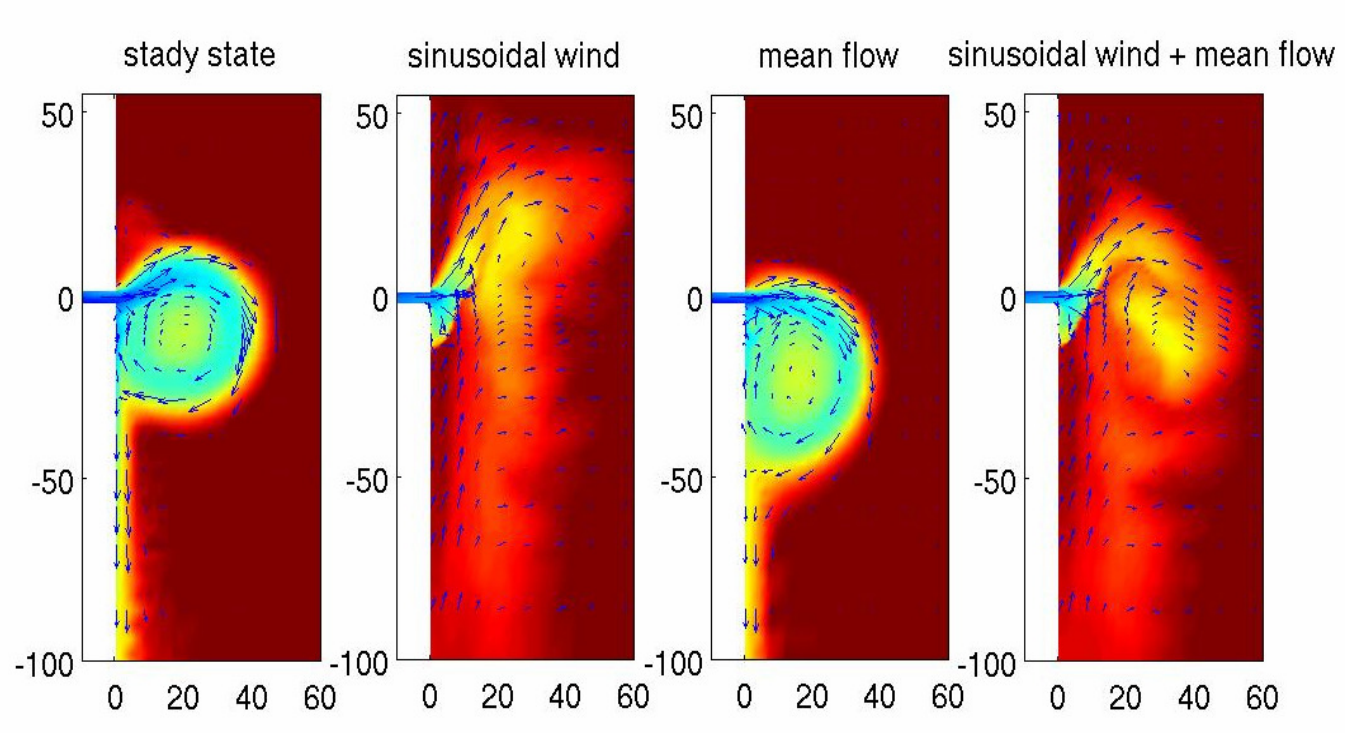

Figure 30. 4 time step figures of 4 difference case during upwelling.

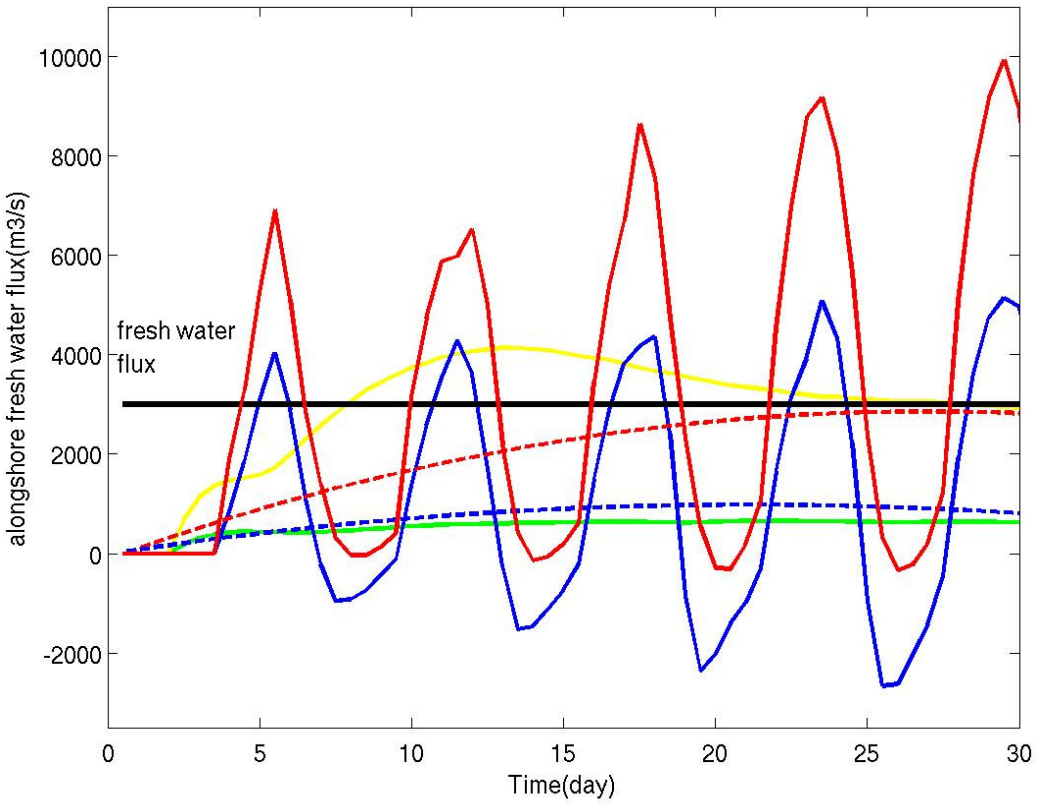

Figure 31. Fresh water flux at 80km from the estuary
black dot: inflow fresh water flux 3000 m^3/s ,
green line: steady state
yellow line: 0.05m/s southward mean flow
blue line: sinusoidal wind
red line: sinusoidal wind + southward mean flow
dot line: running mean.

VITA

Name: Seong-Ho Baek

Address: Department of Oceanography, College of Geosciences, Texas A&M University, 3146 TAMU, College Station, TX 77843-3146, Phone: (979)845-7211, Fax: (979)845-6331

Email Address: Lorense@hanmail.net

Education: B.S., Oceanography, Naval Academy, Republic of Korea, 1994

M.S., Ocean Engineering, Advanced Institute of Military Science and Technology, Republic of Korea, 1997

Ph.D. Oceanography, Texas A&M University, 2006